



Halide Perovskites for Photoelectrochemical Water Splitting and CO₂ Reduction: Challenges and Opportunities

Krzysztof Bienkowski, Renata Solarska,* Linh Trinh, Justyna Widera-Kalinowska, Basheer Al-Anesi, Maning Liu, G. Krishnamurthy Grandhi, Paola Vivo,* Burcu Oral, Beyza Yilmaz, and Ramazan Yıldırım*



Cite This: ACS Catal. 2024, 14, 6603–6622



Read Online

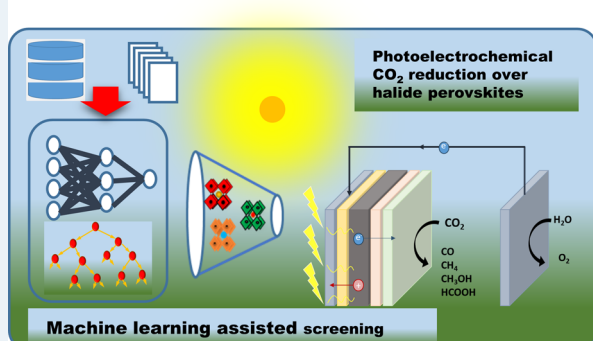
ACCESS |

Metrics & More

Article Recommendations

ABSTRACT: Photoelectrochemical water splitting and CO₂ reduction provide an attractive route to produce solar fuels while reducing the level of CO₂ emissions. Metal halide perovskites (MHPs) have been extensively studied for this purpose in recent years due to their suitable optoelectronic properties. In this review, we survey the recent achievements in the field. After a brief introduction to photoelectrochemical (PEC) processes, we discussed the properties, synthesis, and application of MHPs in this context. We also survey the state-of-the-art findings regarding significant achievements in performance, and developments in addressing the major challenges of toxicity and instability toward water. Efforts have been made to replace the toxic Pb with less toxic materials like Sn, Ge, Sb, and Bi. The stability toward water has been also improved by using various methods such as compositional engineering, 2D/3D perovskite structures, surface passivation, the use of protective layers, and encapsulation. In the last part, considering the experience gained in photovoltaic applications, we provided our perspective for the future challenges and opportunities. We place special emphasis on the improvement of stability as the major challenge and the potential contribution of machine learning to identify the most suitable formulation for halide perovskites with desired properties.

KEYWORDS: photoelectrochemistry, halide perovskites, CO₂ reduction, solar energy conversion, machine learning



1. INTRODUCTION

Given the rapid depletion of fossil fuels and the global energy crisis, solar energy stands out as an attractive renewable energy source. Photocatalytic and photoelectrochemical processes such as water splitting and CO₂ reduction provide an attractive route to utilize solar energy to produce H₂, an energy carrier with great potential for the future, while reducing CO₂ emissions. However, these processes require a catalyst, which is the most sensitive and challenging element in the whole value chain of the activation of small molecules such as H₂O or CO₂, involving the transfer of many electrons and protons. The development of stable photocatalytic structures that combine active site functionality, reaction rate, and intrinsic stability provides a gateway to multielectron activation and subsequent transformation of small molecules such as H₂O or CO₂.^{1–6} In addition, the electron structure dictating the charge transfer efficiency and the surface properties responsible for the activation of substrate molecules are crucial to the overall performance of the working system. Key shortcomings identified by recent studies include: (i) the inability of the materials to trigger and exploit the transfer of multiple charges to reactive sites, (ii) the inability to mimic the chemical

environment more distant from the active site, which is important in controlling the access of reactants to the active site, (iii) the difficulty in lowering the free energy of the transition state, (iv) the inability to induce asymmetric charge distribution in a controlled manner to enhance the efficiency and selectivity of photoelectrochemical (PEC) water splitting and CO₂ reduction processes. Metal halide perovskite (MHP) semiconductors, with their three-dimensional (3D) structure consisting of a [BX₆] octahedral split at the corners, with A-cations occupying 12-fold cubooctahedral voids in the 3D lattice, and in particular, the associated high degree of symmetry, have demonstrated exceptional optoelectronic properties.^{7–16} These include, but are not limited to, high absorption coefficient, band tunability across the visible spectrum (400–800 nm), high carrier conductivity (1–10

Received: December 12, 2023

Revised: March 29, 2024

Accepted: March 29, 2024

Published: April 16, 2024



$\text{cm}^2 \text{ V}^{-1} \text{ s}^{-1}$), long carrier lifetimes, and long charge diffusion lengths ($\sim 1 \mu\text{m}$).^{17–20} Such a unique combination of intrinsic properties of MHP semiconductors has led to the development of promising optoelectronic devices, such as photovoltaics, light emitting diodes, lasers, and photodetectors. More recently, MHPs have also been used in photocatalytic applications.

Halide perovskites, thanks to their 3D structure and a crystal lattice flexible to multiple structural modifications, can enable efficient transport of charges in the bulk and on the surface providing an alternative solution toward efficient and rapid water splitting as well as CO_2 reduction. However, the stability of MHPs, especially toward water, which is the key issue in terms of long-lasting and efficient PEC processes, is a serious concern. Various approaches, such as the use of more stable components (especially cations) and structures (for example, monocrystalline structure), surface passivation, or encapsulations, have been employed to improve the stability of MHPs, often affecting the MHPs' toxicity and band gap simultaneously. Consequently, as reviewed below, numerous works on photoelectrochemical application of halide perovskites have been reported in various papers in recent years, while some review papers covering various aspects of the subject have been also published. For example, Shyamal et al.²¹ reviewed the photocatalytic CO_2 reduction over halide perovskite nanocrystals, and Chen et al.²² reviewed the applications of these materials in both in water splitting and CO_2 reduction in 2020. Similar works have been continued to be published in recent years covering CO_2 reduction²³ or water splitting and CO_2 reduction²⁴ together. In one of the more recent works, Wang et al.²⁵ extensively reviewed the synthesis and use of halide perovskites for CO_2 reduction while Chen et al.²⁶ discussed the strategies to improve the stability and photocatalytic activity of halide perovskites.

In addition to the experimental works in the field, machine learning (ML) has also been used extensively in recent years for accelerating the discovery of new MHPs with desirable properties (especially stability and band gap) for visible light harvesting. Density functional theory (DFT) simulations (sometimes together with ML) have also been used to identify novel MHP compositions and understand their optoelectronic properties. The ML screening of DFT generated MHPs data has also been extensively employed in recent years. The accumulation of a large amount of data/knowledge on these materials due to their widespread use in photovoltaics since the 2010s, the presence of a large number of alternative structures that can be formed by changing the anion, cation, and their ratios, and the need for stable and safe but still sufficiently efficient structures made ML/DFT-assisted screening an effective route to discovering new halide perovskites with improved properties. Consequently, numerous research papers, including several reviews, have been published on ML applications of halide perovskites. Although most of the works published so far have focused on halide perovskites solar cells, the experience gained in the field will be also beneficial for PEC applications as well because the visible light harvesting efficiency and stability are also the major performance measures in PEC applications, which have also been presented in the scientific literature more frequently in recent years due to the progress achieved in the water resistance of halide perovskites.^{27–30}

The scope of this review is to discuss the current state-of-the-art metal halide perovskites in relation to the key

limitations of PEC water splitting and photoelectrochemical CO_2 reduction, which need to be addressed in order to achieve substantial efficiency improvements for these processes. Herein, we present a critical assessment of the application of various MHP semiconductors, the challenges related to their poor stability, and future opportunities leveraging the massive experience in MHP photovoltaics. We think that our work is novel in several aspects and will make significant contribution to the field. We covered all relevant issues of the subject, including the synthesis of halide perovskites and their utilization in photoelectrochemical water splitting and CO_2 reduction, while especially focusing on the recent developments to improve the stability of halide perovskites (especially against water), which is a major challenge in utilization of these materials in photoelectrochemical processes. Another important characteristic of halide perovskites is that they can be in large variety of configurations considering the large number of alternatives for A, B, and X sites. However, the number of synthesizable and stable structures with suitable electronic properties is limited; hence, the use of machine learning to discover or design new halide perovskite structures constitutes an important part of efforts toward the effective use of halide perovskites in photoelectrochemical reactions. Consequently, as different from similar reviews in the literature, we also covered the ML applications in the field and provided a future perspective for the utilization of this important tool in photoelectrochemical applications of halide perovskites.

2. SOLAR DRIVEN PROCESSES: CURRENT STATE OF ART IN PEC WATER SPLITTING AND CO_2 REDUCTION

2.1. PEC Water Splitting. As of today, various semiconducting materials such as metal oxides, metal sulfides, and metal nitrides including TiO_2 ,^{31–33} WO_3 ,^{34,35} Cu_2O ,^{36,37} CuO ,³⁸ BiVO_4 ,^{39,40} Fe_2O_3 ,^{41,42} CdSe ,⁴³ CdS ,^{44,45} Ta_3N_5 ,⁴⁶ and C_3N_4 ^{47–49} have been investigated for water splitting in PEC cells. However, the photocatalytic activity of these materials is often limited due to the sluggish kinetics of oxygen evolution or too positive potential of the conduction band to drive hydrogen evolution. The reaction of oxygen formation through water oxidation, which is a necessary semireaction toward hydrogen realization, is thermodynamically and kinetically demanding. Consequently, a small number of electrons can react in the reduction reaction to form H_2 ($2\text{H}^+ + 2\text{e}^- \rightarrow \text{H}_2$), due to the recombination of photo-generated h^+ and e^- ; only a small number of these electrons would be able to reach the semiconductor surface, where the reaction takes place. The band gap energy of the conduction band (CB) should be more negative than the potential for the hydrogen evolution reaction (HER) (0 eV) and the band gap position of the valence band (VB) more positive than that for the oxygen evolution reaction (OER) (1.23 eV), and although they can produce hydrogen and oxygen, they can also react with water causing back reactions, which in turn reduces the overall efficiency of the photocatalytic process. Finally, semiconductor materials often suffer from poor absorption of visible light due to their band gap width and electronic structure. Furthermore, the efficiency of the solar-to-hydrogen/hydrogen-to-hydrogen (STH) conversion process is highly dependent on the chemical stability of the semiconductors, which can be affected by many factors, such as pH, halogen introduction, interference ions, and so on. Various strategies have been proposed, including the use of new and more

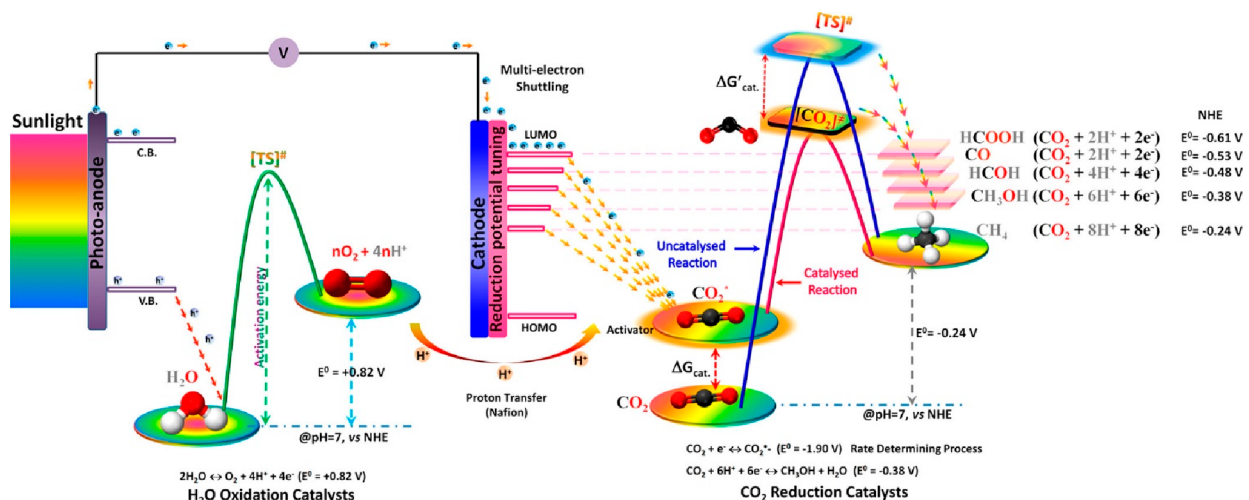


Figure 1. Schematics illustrating the band gap energetics involved in the water oxidation and CO₂ reduction reactions in PEC and the role of the activation catalyst in thermodynamic and kinetic terms. The symbols “*” and “‡” represent the activated state and the transition state of CO₂ by adsorption on the cathode surface, respectively. Reproduced with permission from ref 68. Copyright 2019 American Chemical Society.

efficient semiconductors like MHPs, heterojunction design through the use of a cocatalyst on the semiconductors to improve light-harvesting efficiency, promote the charge separation process, and provide a protective layer for the underlying substrate materials.

The most important aspect of efficient charge separation and transfer from the semiconductor to the cocatalyst is the engineering of a suitable semiconductor/cocatalyst heterojunction.⁵⁰ In addition, cocatalysts can provide a lower overpotential for the reduction of water molecules compared to photocatalysts.⁴⁸ Furthermore, appropriate band alignment of the formed heterojunctions can improve visible light harvesting.⁵¹ Historically, water oxidation catalysts have been based on noble metal materials as the large-scale implementation has been hampered by the limited availability and cost of these metals.⁵² Hence, the development of nonprecious and metal-free materials is essential. Low-cost and earth-occurring transition metals such as Cu,^{53–57} Ni,⁵⁸ and Co^{59,60} are examples of nonprecious elements that have been successfully used as cocatalysts in HER. Carbon-based supports such as graphitic carbon nitride (g-C₃N₄), graphene and its derivatives,^{61–63} as well as an organohydride-catalyst⁶⁴ may also enhance photocatalytic CO₂ reduction performance by overcoming the limitation faced by a traditional photocatalyst through their suitable physiochemical and electrical properties like high surface area, stability, anticorrosion capacity, photosensitivity, and conductivity.

While there are many solutions and approaches to overcome the slow oxygen formation in PEC water splitting, one common problem that needs consideration lies in multi-electron reactions and the need for long-lived holes on the surface.⁶⁵ The latter is determined by the efficient transport of charges in the bulk and on the surface, which is why halide perovskites, thanks to a crystal lattice flexible to multiple structural modifications, can provide an alternative solution toward efficient and rapid water splitting.

In summary, the goal is not to find a semiconductor that can do both CO₂ reduction and O₂ evolution but to find complementary light absorbers for both reactions. As we reviewed in Section 3, MHPs may be the potential solution for low efficiency of the PEC water splitting process even though

they have their own challenges to overcome as we summarized in Section 4.

2.2. Photoelectrochemical (PEC) CO₂ Reduction. PEC CO₂ reduction has the following advantages over other electrochemical approaches: (i) significantly reduced overpotential required for uphill processes, (ii) relatively low cost of cell construction and operation, (iii) modulated, through applied potential, product selectivity and distribution, (iv) tuned band gap energetics that are useful parameters to help reduce CO₂ activation energy. However, before running any reduction system, a key question must be answered: how does one activate the inert CO₂ molecule? Figure 1 illustrates a schematic of the thermodynamic energy levels required to be overcome prior to the start of the water splitting or CO₂ reduction reaction in a PEC cell, in the presence and absence of a catalyst. The green curve is assigned to the activation energy required for the water splitting reaction and illustrates the oxidation reaction of water with proton production passing from the H₂O to the O₂ energy level. The red and blue lines are for the CO₂ reduction reaction and represent the activation energy curves in the presence or absence of catalysts, respectively. As can be seen in the diagram, electron transfer can help reduce the activation energy of the CO₂ reduction reaction if a suitable electron transfer accelerator (e.g., a metal plasmon) is used.⁶⁶ The overall CO₂ reduction reaction can be achieved by combining electrons with appropriate energy levels, which are necessary for the activation and subsequent reduction of CO₂. To obtain better product selectivity, CB and VB positions of the photocatalyst should be fully aligned. The major difficulty is to find a pristine semiconductor material with the right band gap energy position to suit both processes, namely the CO₂ reduction and the water oxidation reaction.⁶⁷

Although great progress has already been made, there are still areas of concern for CO₂ reduction in PEC cells, such as (i) insufficient light absorption, (ii) inefficient charge separation and transport, and (iii) slow catalytic conversion at the surface. There are two main factors affecting the extent of light absorption by a photocatalytic material; the bandwidth and surface properties of the semiconductor materials used. Planar semiconductors show a relatively low light absorption efficiency due to their high surface reflectance. In general,

inadequate light absorption is the main problem responsible for the reduction in total energy conversion efficiency, creating a need for new semiconductors like MHPs with high visible light harvesting capabilities. In addition, the total energy conversion efficiency is even more negatively affected by strong recombination processes of photoexcited charge carriers due to surface states, impurities or defects.⁶⁹ The quality of the interface and its electron structure affect the transport of minority carriers toward the surface, which can be inhibited by a weak embedded electric field. Last but not least, surface catalytic conversion is challenging due to the complex electrochemistry of CO₂ reduction. Due to the two stable, difficult-to-activate and dissociate C=O bonds present in the CO₂ molecule, a large overpotential is required to overcome the CO₂ reduction reaction barrier, as observed in the slow electrochemical kinetics of CO₂ reduction compared to the competitive HER.^{70–72} Furthermore, CO₂ reduction can occur via several possible reaction pathways, resulting in a low reaction selectivity. The introduction of suitable cocatalysts could increase activity and improve conversion selectivity.

Although noble-metal-based cocatalysts are the most widely used and can help achieve high CO₂ conversion efficiencies (CO being the main product), as they do in water splitting, their rarity and high cost severely limit their large-scale use. However, highly abundant materials such as Cu-based catalysts used in PEC-based CO₂ reduction for hydrocarbons and alcohols do not offer good product selectivity. Even though the use of biological cocatalysts avoids side reactions and gives high selectivity for a specific product, their large-scale use is also limited due to their high cost and poor stability under light irradiation. Reports on the use of carbonaceous materials in CO₂ reduction by PEC processes are rare. Yet, there are very promising carbonaceous candidates as ideal cocatalysts. Their unique surface configurations and large active surfaces facilitate efficient adsorption and activation of CO₂ molecules yielding high CO₂ reduction efficiencies.⁷³

3. HALIDE PEROVSKITES

3.1. General Overview. The first synthetic perovskite oxide, CaTiO₃, was synthesized in 1851 using a flux growth process.⁷⁴ Later on, the first MHPs, with composition CsPbX₃ (X = Br, Cl, I), were synthesized from aqueous solution by Wells et al. as early as 1893,^{75,76} but their perovskite structure was confirmed in 1957 by Møller.⁷⁵ The first organometallic halide perovskites with methylammonium as the A-site cation were synthesized by Weber and co-workers two decades later (1978).⁷⁷ In a typical MHP, the A-site of the ABX₃ structure (Figure 2a) can be occupied by inorganic monovalent cations (such as cesium in CsPbI₃), organic cations (such as methylammonium or formamidinium in MAPbI₃ and FAPbI₃, respectively), or hybrid organic–inorganic monovalent cations (Cs_x(MA_{0.17}FA_{0.83})_(1-x)Pb(I_{0.83}Br_{0.17})₃, with x = 5%). The B site is occupied by an inorganic divalent cation, such as Pb²⁺, Sn²⁺, or Ge²⁺. Finally, the X site is occupied by a halide anion (Br⁻, Cl⁻, and I⁻) or by a combination of these anions. The cubic crystal structure of ABX₃ is given in Figure 2b. Recently, MHPs have become extremely popular due to intensive research into their synthesis, compositional engineering, and applications. MHPs exhibit remarkable optical properties, including a high optical absorption coefficient and the ability to absorb light across a broad spectrum ranging from the visible to the near-infrared region of the electromagnetic spectrum. Additionally, the band gaps of perovskites

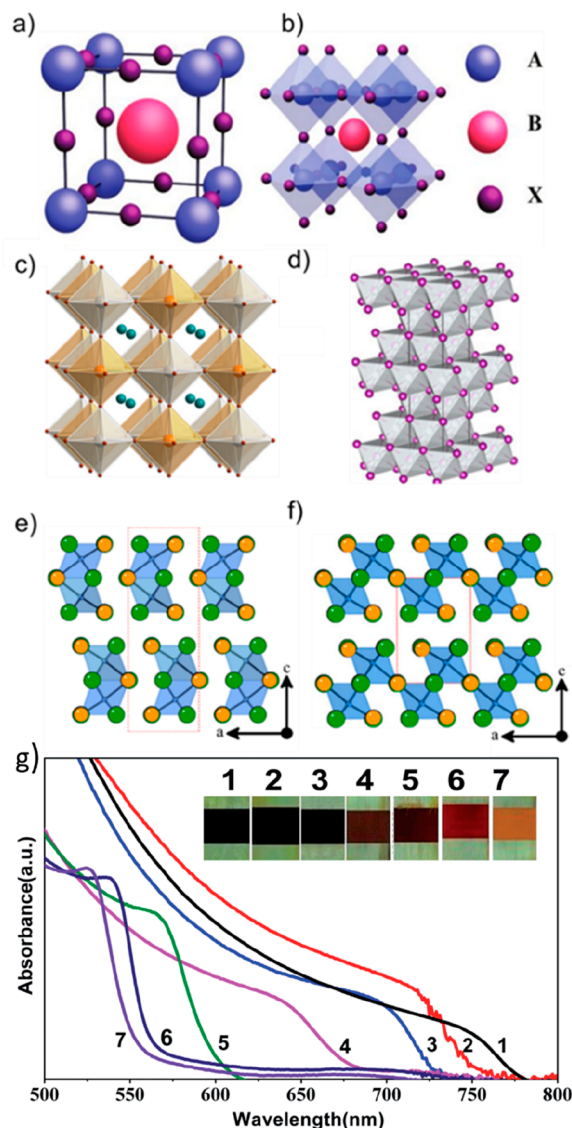


Figure 2. (a) Unit cell of deal cubic ABX₃ perovskite, and (b) ABX₃ cubic perovskite crystal structure. Reproduced with permission from ref 112. Copyright 2018 Wiley. (c) Crystal structure of A₂B'BX₆ double perovskites. Orange for B, gray for B', turquoise for A, and brown for X. Reproduced with permission from ref 113. Copyright 2016 American Chemical Society. (d) Crystal structure of the A_aB_bX_x halide ruddrites. Reproduced with permission from ref 104. Copyright 2017 Wiley. (e) Crystal structure of 0D A₃B₂X₉ nonperovskite. (f) 2D layered structure of A₃B₂X₉ vacancy-ordered perovskite. Orange for A, green for X, and blue for B. Reproduced with permission from ref 109. Copyright 2015 American Chemical Society. (g) UV-vis absorption spectra of mixed halide lead perovskite (MAPb(I_{1-x}Br_x)₃) films. The numbers 1–7 denote samples corresponding with increasing bromine content (X) within the films. Reproduced with permission from ref 81. Copyright 2014 Royal Society of Chemistry.

can be easily tuned through chemical composition engineering. The defect-tolerant nature of MHPs allows for large carrier diffusion lengths (~ 100 nm – ~ 1 μ m) for polycrystalline film and to over 100 μ m for single crystals.^{11,78,79} MHPs typically exhibit low exciton binding energies, which means that low energy is required for exciton dissociation into free charge carriers (electrons and holes), indicative of efficient charge separation.⁸⁰ Band gap tunability can be achieved through

partial or full substitution at the halide site or A-site cation. For instance, replacing iodide with bromide in MAPbI_3 may lead to a blue shift of band edge and increase the band gap (Figure 2g),⁸¹ while substituting MA with FA may lead to a red shift and decrease of the band edge.⁸² This band gap tunability along with other outstanding optical properties of MHPs enable the control of perovskite properties for various optoelectronic applications.

The structural dimensionality of a material is related to the atoms' arrangement and connections, which affect the crystal structure, bonding types, and defects of the material. MHPs can exist in various structural dimensionalities, including 3D, 2D, 1D, and 0D. In contrast, the electronic dimensionality describes the connection between the atomic orbitals comprising the lower conduction band (LCB) and upper valence band (UVB), which impact the material's band gap and carrier transport.^{9,83} Due to the isolation of the octahedra, in materials with 0D electronic dimensions, the LCB and UVB are nondispersive in all directions and the electrons are confined within all three spatial dimensions, producing distinct energy levels and quantum phenomena. Cs_4PbBr_6 , exhibiting a 0D both in its electronic and structural dimensions, comprises isolated $[\text{PbBr}_6]^{4-}$ octahedra isolated by Cs^+ ions. In comparison with its 3D counterpart, 0D Cs_4PbBr_6 exhibits a hundred times higher photoluminescence quantum yield⁸⁴ due to large exciton binding energy.⁸⁵ In the case of MHPs with 1D electronic and structure dimensions, the CBM and VBM overlap only along the chains of octahedra but not perpendicularly, and the electron motion is thus confined to one direction. Consequently, the LCB and UVB are narrower, resulting in a larger band gap than that of their 3D and 2D counterparts.^{9,86} In 2D MHPs, the organic cations act as insulating spacers, and electrons are allowed to move within two dimensions and are confined in the third dimension. In comparison to 3D perovskites, the presence of organic spacers in 2D perovskites enhances the ambient stability and affects the structural distortion that can control the band edge states.^{87,88}

Although many materials that possess 3D structures may be electronically 3D, having a 3D structure does not guarantee electronic three-dimensionality and vice versa. The mismatch between the structural and electronic dimensions is clearly visible in the lead-free double halide perovskite $\text{Cs}_2\text{AgBiBr}_6$ (Figure 2c). This material, despite its 3D structure, is electronically low dimensional (LD) and has an indirect band gap.^{89,90} The large intermediate band gap and low electronic dimensionality of $\text{Cs}_2\text{AgBiX}_6$ were found to be due to the orbital mismatch between Ag and Bi.^{15,91} The transition from an indirect to a direct band gap for $\text{Cs}_2\text{AgBiBr}_6$ can be achieved by lowering the structural dimensionality with specific organic spacer cations, such as butylammonium, allowing for a layered 2D crystal structure.¹⁴ However, LD structures also have low electronic dimensionality, leading to large band gaps and large effective carrier masses.^{89,90}

Notwithstanding the excellent intrinsic properties of lead halide perovskites (LHPs) that make promising semiconductors, the toxicity and instability are by far the biggest challenges to be urgently addressed.^{92,93} Researchers have explored low-toxicity alternatives, such as divalent metal cations like germanium (Ge^{2+}) and tin (Sn^{2+}), to replace Pb^{2+} and retain the perovskite crystal structure of ABX_3 . These lead-free materials are called 3D perovskite-like materials.^{17,94} Sn^{2+} -based perovskites, such as MASnI_3 , CsSnI_3 , have direct band

gaps between 1.2 and 1.4 eV.^{94–96} On another hand, Ge^{2+} -based structures, like CsGeI_3 , MGeI_3 , and FAGeI_3 , show direct band gaps between 1.6 and 2.4 eV.⁹⁷ However, both Ge and Sn suffer from rapid oxidation when exposed to the ambient air.^{17,97} Since $\text{Sn}^{2+}/\text{Sn}^{4+}$ has a low redox potential (-0.15 V), Sn^{2+} is easily oxidized to Sn^{4+} when exposed to air, and this process is accelerated by the presence of H_2O . The presence of Sn^{4+} leads to the destruction of the perovskite structure, which adversely affects the stability of the material.^{98,99} Like Sn^{2+} , Ge^{2+} is not stable and tends to oxidize to the stable Ge^{4+} following the same trend as the Sn^{2+} -based perovskite. Therefore, finding low-toxicity and stable absorption materials is of great interest. The replacement of the cations in the A-site by larger organic cations, e.g., butylammonium (BA) and 2-phenyl-ethylammonium (PEA), in Ge^{2+} - and Sn^{2+} -based perovskite results in a low dimensionality structure and a widening of the direct band gap to (>2). $(\text{PEA})_2\text{SnI}_4$ and $(\text{PEA})_2\text{GeI}_4$ exhibit 2D perovskite structures and have high stability to oxidation compared to 3D counterpart perovskites.^{100,101}

Antimony (Sb) and bismuth (Bi) are of great interest as lead-free perovskite-inspired materials (PIMs) because both Bi^{3+} and Sb^{3+} have electron structures similar to those of Pb^{2+} and are less toxic than lead, more stable, and abundant enough for large-scale use. Their electronic structure is responsible for the interesting optoelectronic properties. PIMs may not have the same crystal structure and/or ABX_3 composition, like LHPs. Indeed, the replacement of lead by Bi^{3+} or Sb^{3+} results in a low-dimensional structure, differing from the three-dimensional structure of ABX_3 perovskites.^{102,103}

Among the various perovskite-inspired materials, iodobismuthates, 2D layered structures, and nonperovskite 0D structures have received widespread attention as potential lead-based alternatives, especially for photovoltaic applications. Iodobismuthates, often crystallizing in the NaVO_2 rudorffite structure, are a class of PIMs based on the ternary $\text{Ag}-\text{Bi}-\text{I}$ system with the general formula of $\text{Ag}_a\text{Bi}_b\text{X}_{a+b}$. Rudorffites (Figure 2d) have 3D structures based on edge-shared octahedra $[\text{AX}_6]$ and $[\text{BX}_6]$ octahedra and have direct band gaps of <2 eV.¹⁰⁴ Several rudorffite materials have been investigated for photovoltaic application, such as AgBi_2I_7 , Ag_3Bi_6 ,¹⁰⁴ AgBiI_4 ,^{106,107} and Ag_2BiI_5 .

Bi^{3+} or Sb^{3+} compounds with the $\text{A}_3\text{B}_2\text{X}_9$ chemical composition crystallize in 2D perovskite or 0D nonperovskite polymorphs, depending on the preparation method. The 2D layered structure of $\text{A}_3\text{B}_2(\text{V})\text{X}_9$ is also known as vacancy-ordered perovskite, in which the ratio of B-site cations to vacancies is 2:1 while the 0D structure consists of pairs of isolated face-sharing $[\text{B}_2\text{I}_9]^{3-}$ octahedra is surrounded by A.¹⁰⁸ Starting from the most common example of $\text{A}_3\text{B}_2\text{X}_9$, $\text{Cs}_3\text{Sb}_2\text{I}_9$ exhibited both 2D layered perovskite (Figure 2f) and 0D nonperovskite structure (Figure 2e); while the layered 2D perovskite structure is formed by vapor deposition, the 0D nonperovskite structure is easily produced via solution processing.¹⁰⁹ 0D $\text{Cs}_3\text{Sb}_2\text{I}_9$ is thermodynamically more favorable in synthesis than 2D, but 2D $\text{Cs}_3\text{Sb}_2\text{I}_9$ shows greater potential for optoelectronic properties than 0D.^{109,110} The 0D/2D $\text{Cs}_3\text{Sb}_2\text{I}_9$, 2D $\text{MA}_3\text{Sb}_2\text{I}_9$, 0D $\text{Cs}_3\text{Bi}_2\text{I}_9$, and 0D $\text{MA}_3\text{Bi}_2\text{I}_9$ are the most studied compounds of the $\text{A}_3\text{B}_2\text{I}_9$ class of materials.^{109,111}

Synthesizing polycrystalline MHPs can be achieved through either solution deposition or vacuum deposition methods. Solution deposition involves using various techniques such as

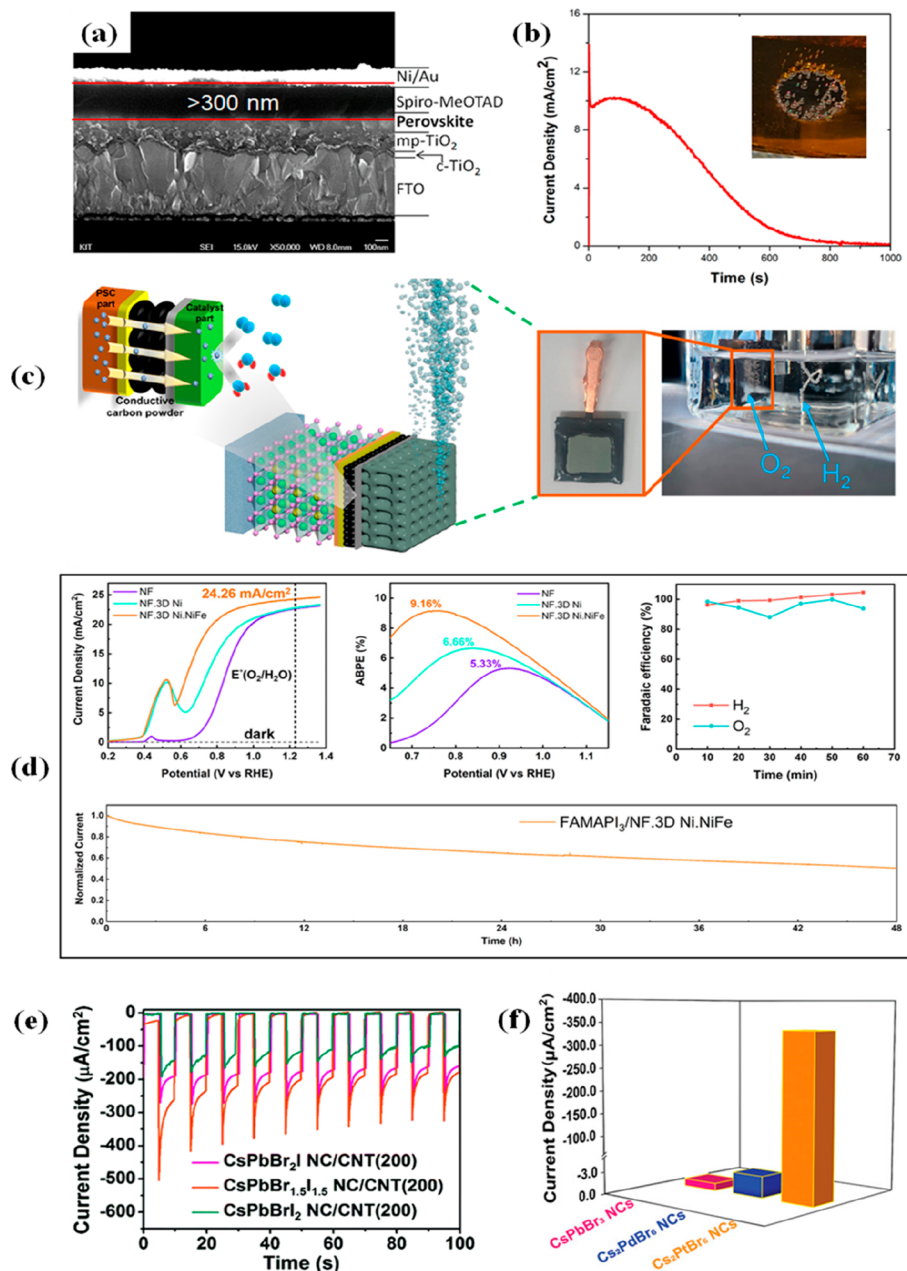


Figure 3. (a) SEM cross-sectional image of the MAPbI₃-based photoanode. (b) Photocurrent density vs time graph of perovskite photoanode under illumination (0.7 sun) and bias (1.0 V vs SHE). Reproduced with permission from ref 131. Copyright 2016 American Chemical Society. (c) Schematic illustration (left) and photo (right) of the perovskite photoanode configuration for PEC O_2 evolution.¹³⁴ (d) Top left: Photocurrent density; top middle: applied bias photon-to-current conversion efficiency (ABPE), and top right: faradaic efficiency of the FAMAPbI₃-based photoanode. Reproduced with permission from ref 134. Copyright 2022 American Chemical Society. (e) Amperometric $I-t$ curves of the CsPbBr_xI_{3-x} NC/carbon nanotube at -0.4 V. Reproduced with permission from ref 135. Copyright 2019 Royal Society of Chemistry. (f) Current densities of different halide perovskite nanocrystal-based PEC systems. Reproduced with permission from ref 137. Copyright 2021 Wiley-VCH.

spin-coating, drop-casting, hydrothermal synthesis, solvothermal synthesis, ultrasound-assisted synthesis, and microwave-assisted synthesis to create thin films from precursor solutions. On the other hand, vacuum deposition methods involve synthesizing MHPs through coevaporation under high vacuum conditions. Vacuum deposition methods can be further categorized into thermal evaporation, pulsed laser deposition, and chemical vapor deposition, whereas the colloidal nanocrystal can be synthesized by hot-injection and ligand-assisted reprecipitation.^{114–116}

3.2. Halide Perovskite for Water Splitting. Over the past decade, halide perovskites led to unprecedented advances in a variety of optoelectronic applications, such as solar cells,¹¹⁷ light-emitting diodes (LEDs),¹¹⁸ photodetectors,¹¹⁹ and PEC water splitting with an increasing interest.¹²⁰ Similar to conventional PEC cells using metal oxides (e.g., TiO₂ or WO₃) as the photoelectrode, a typical halide perovskite PEC cell consists of a working electrode (WE) (i.e., a halide perovskite-based photoelectrode), a counter electrode (CE), and a reference electrode (RE). This type of photoelectrode

structure effectively solves the critical stability problems of halide perovskites immersed in aqueous electrolytes by easily covering a waterproof and conductive protective layer on top of the halide perovskite layer. To date, many efforts have been made to stabilize halide perovskite photoelectrodes by depositing different types of such protective layers, e.g., Ni thin films (~ 8 nm), field metal (FM),¹²¹ Ti foil,¹²² graphite epoxy^{123,124} or pyrolytic graphite,¹²⁵ and carbon-based coating layers^{126–128} on halide perovskite photoanodes in the n-i-p structure or halide perovskite photocathodes in the p-i-n counterpart.

In the following section, we briefly introduced the fabrication of PEC cells based on halide perovskites in both thin films and nanocrystals, which are classified in terms of target reactions, i.e., the evolution of oxygen and the evolution of hydrogen, respectively.

3.2.1. Halide Perovskite-Based Photoanodes for Oxygen Evolution. To reach oxygen evolution by photoelectrochemical oxidation of water, PEC cells with halide perovskites in n-and-p configuration are used as photoanodes. Typically, photo-generated holes in the perovskite layer are transported to the corresponding electrode via hole-transport layers (HTLs), which oxidize oxygen ions supplied by the aqueous electrolyte. As described above, the high susceptibility of halide perovskites to water is considered as one of the major barriers for their use in PEC cells. To date, significant research has been conducted to protect halide perovskite-based photoelectrodes within PEC cells by coating them with a water-resistant and ideally electrocatalytic layer. In 2015, Da and co-workers¹²⁹ assembled, for the first time, a $\text{CH}_3\text{NH}_3\text{PbI}_3$ (MAPbI₃)-based multilayer photoanode coated with an ultrathin Ni layer (~ 8 nm), which serves as both a waterproof shield and Ohmic contact.

A record photocurrent density of >10 mA cm⁻² was achieved in 0.1 M Na₂S at 0 V_{Ag/AgCl} under 1 sun illumination (100 mW cm⁻²), and it retained >2 mA cm⁻² after 15–20 min of illumination using bias. This finding indicated that the Ni thin film could be a promising candidate as a protective catalytic layer for halide perovskite photoelectrodes to be used in water splitting reactions. Wang and co-workers¹³⁰ further improved the stability of the MAPbI₃-based PEC system using both Ni-coating and functionalization of the perovskite surface with hydrophobic alkylammonium cations (tetraethylammonium (TEA) and tetrabutylammonium (TBA)). The TEA-treated perovskite photoanodes can sustain PEC water oxidation for about 30 min but with an unexpectedly low photocurrent density of 2 mA cm⁻², which is probably attributed to a decrease in the conductivity of the protective layers. On the other hand, many holes were created on the surface of the perovskite after TBA treatment, resulting in incomplete Ni coverage and thus a decrease in PEC efficiency (photocurrent of only 0.42 mA cm⁻²); it is important to achieve a morphology without holes on top of the perovskite layer, which can effectively impede water penetration. Hoang and co-workers¹³¹ fabricated a MAPbI₃-based photoelectrode with a thick (>300 nm, see cross-sectional SEM image in Figure 3a) and dense spiro-OMeTAD HTL, which greatly improves the stability of the perovskite photoanode with a long lifetime of almost 60 min (Figure 3b) while maintaining the water oxidation reaction.

Later in 2018, the same group¹³² used a mold-cast and life-off process to introduce a low-melting-point Field's metal (FM) layer sandwiched by a perovskite layer and Ni shielding,

which strikingly stabilizes the perovskite photoanode in a harsh oxidative environment for more than 10 h. As the FM lacks catalyst activity for oxygen evolution, the authors optimized a thickness of ~ 10 μm for the catalytic Ni layer, achieving a constant photocurrent of 13 mA cm⁻² for about 6 h under illumination (0.7 sun), as well as a bias of 1.3 V_{RHE} (RHE = reversible hydrogen electrode) in a KOH electrolyte.

As an alternative to metal-based shielding, low-cost carbon-based materials have also been used as excellent protective layers as well as electrocatalytic layers by insulating the perovskite from the aqueous solution. For instance, Tao and coauthors¹³³ used a mixed cationic perovskite (S-AVA)_x(MA)_{1-x}PbI₃ [$\text{S-AVA} = \text{HOOC}(\text{CH}_2)_4\text{NH}_3^+$]-based photoanode encapsulated with conductive carbon paste and silver coating for both as water-resistant and hole transporting medium; they achieved a high photocurrent density of 12.4 mA cm⁻² at 1.23 V_{RHE} in a KOH solution under 1 sun illumination, while demonstrating the unprecedented stability that PEC performance can be continuously maintained with a steady-state response for >12 h. It is well-known that the implementation of water splitting should meet the operational requirement of 1.23 V. Therefore, halogen perovskites with a wide bandwidth, e.g., CsPbBr₃, have recently attracted more attention for application in PEC cells. Poli and co-workers constructed a TiO₂|CsPbBr₃|mesoporous carbon (m-c)|graphite plate (GS) photoanode, demonstrating a constant photocurrent of over 2 mA cm⁻² at 1.23 V_{RHE} under continuous illumination (AM 1.5 G) with an outstanding stability of >30 h in a liquid electrolyte. More interestingly, the authors modified the GS with an Ir-based water oxidation catalyst (WOC), which led to a decrease in E_{onset} (initial potential) of about 100 mV with increased photovoltage (>1.3 V). More recently, Kim and co-workers¹³⁴ used conductive carbon powder (CCP) as a coupler between a monolithic photodiode based on double cationic perovskite (FA_{0.93}MA_{0.07}PbI₃) and a robust NiFe-layered Ni film catalyst (Figure 3c). The fabricated perovskite photoelectrode shows an E_{onset} of 0.56 V and an extremely high photocurrent density of >24 mA cm⁻² at 1.23 V_{RHE}, with a promising photocurrent efficiency (ABPE) of 9.16% (see Figure 3d). This work also highlights an extremely stable lifetime of 48 h for the PEC performance under constant illumination.

Compared to the widespread use of bulk 3D halide perovskite layers in PEC cells, the use of nanocrystalline (NC) perovskite-based layers as photoelectrodes is still in its infancy due to the difficulty of fabricating high-quality NCs perovskite layers as well as high water susceptibility. In contrast, their suspension-phase counterparts have been extensively studied for conventional photocatalytic reactions. Yang and co-workers¹³⁵ investigated the photoelectrochemical activity of hybrid photoelectrodes based on CsPbBr_{3-x} NCs/carbon nanotubes (CNTs), obtaining a reasonable photocurrent density of 417 μA cm⁻², which shows an almost 8-fold increase compared to the initial CsPbBr₃ NC composite without CNTs at -0.4 V_{Ag/AgCl} under calibrated illumination of 150 mW cm⁻² (see Figure 3e). Furthermore, instead of coating protective surface layers, the development of stable halide perovskites alone is still strongly requested to create sustainable PEC cells.

Lead-free halide perovskites in both bulk and nanocrystal forms have shown their great potential in fulfilling this intrinsic requirement. Hamdan and co-workers¹³⁶ prepared a thin photodiode based on a 3D Cs₂PtI₆ perovskite thin film without

Table 1. Summary of Representative Water Splitting Studies on Halide Perovskite-Based PEC Cells

Reaction type	PEC cell configuration	Electrolyte	Irradiation	Potential	Photocurrent density	Faradic efficiency	Duration	Ref.
Water oxidation	FTO TiO ₂ MAPbI ₃ Spiro-OMeTAD Au Ni	0.1 M Na ₂ S	100 mW cm ⁻² (AM 1.5G)	N/A	>10 mA cm ⁻² @ 0 V _{Ag/AgCl}	N/A	0.25–0.33 h	129
	FTO TEA-modified MAPbI ₃ Spiro-OMeTAD Au Ni	0.1 M Na ₂ S	100 mW cm ⁻² (AM 1.5G)	N/A	2.1 mA cm ⁻² @ 0 V _{Ag/AgCl}	N/A	>0.5 h	130
	FTO c-TiO ₂ Im-TiO ₂ MAPbI ₃ Spiro-OMeTAD Au Ni	K-Borate/1.0 M KOH	0.7 sun illumination	0.5 V _{SHE}	17 mA cm ⁻² @ 1.23 V _{SHE}	N/A	1 h	131
	FTO TiO ₂ MAPbI ₃ Spiro-OMeTAD Au Fe Mn Ni	1.0 M KOH	0.7 sun illumination	0.75 V _{RHE}	13 mA cm ⁻² @ 1.3 V _{RHE}	N/A	6 h	132
	FTO TiO ₂ (S-AVA) _x (MA) _{1-x} PbI ₃ conductive carbon sliver paint carbon	1.0 M KOH	100 mW cm ⁻² (AM 1.5G)	0.8 V _{RHE}	12.4 mA cm ⁻² @ 1.23 V _{RHE}	82%	>48 h	133
	FTO TiO ₂ CsPbBr ₃ Im-carbon graphite sheet Ir-based WOC	0.1 M KNO ₃	100 mW cm ⁻² (AM 1.5G)	0.6 V _{RHE}	2 mA cm ⁻² @ 1.23 V _{RHE}	N/A	30 h	140
	FTO SnO ₂ FA _{0.03} MA _{0.07} PbI ₃ Spiro-OMeTAD Au conductive carbon powder Ni foil (NiFe)	1 M KOH (pH = 14)	100 mW cm ⁻² (AM 1.5G)	1.5 V _{RHE}	24.26 mA cm ⁻² @ 1.23 V _{RHE}	~100%	48 h	134
	FTO CsBr J _x J _{3-x} NC/carbon nanotube	0.1 M TBAPF ₆	150 mW cm ⁻² (AM 1.5G)	N/A	0.417 mA cm ⁻² @ -0.4 V _{Ag/AgCl}	N/A	>0.03 h	135
	FTO TiO ₂ Cs ₂ Pt ₆	1 M KOH (pH = 11)	AM 1.5G	1.1 V _{Ag/AgCl}	0.8 mA cm ⁻² @ 1.23 V _{RHE}	N/A	>12 h	136
	Cs ₂ PtBr ₆ NCl/glassy carbon electrode	0.1 M phosphate buffer solution	10.18 mW cm ⁻² (365–370 nm LED light)	0.5 V _{Ag/AgCl}	0.335 mA cm ⁻² @ -0.6 V _{Ag/AgCl}	N/A	>0.16 h	137
	FTO Cs ₂ CuSb ₂ Cl ₁₂ NC	0.1 M NH ₄ PF ₆	100 mW cm ⁻² (AM 1.5G)	N/A	0.006 mA cm ⁻² @ -0.85 V _{Ag/AgCl}	N/A	>0.16 h	138
	Pt/graphite epoxy CsFAMA FTO glass FTO	0.1 M KBi, 0.1 M K ₂ SO ₄ buffer (pH = 8.5)	100 mW cm ⁻² (AM 1.5G)	1.8 V _{RHE}	15 mA cm ⁻² @ 1.23 V _{RHE}	N/A	96 h	123
	FTO PEDOT:PSS MAPbI ₃ PCBM Ag FM Pt	0.1 M borate	100 mW cm ⁻² (AM 1.5G), λ > 400 nm	0.7 V _{RHE}	9.8 mA cm ⁻² @ 0 V _{RHE}	95.1%	1.8 h	121
	FTO NiO ₃ CsFAMA perovskite PCBM FM Pt-BiVO ₄ TiC _o	0.1 M borate, K ₂ SO ₄	100 mW cm ⁻² (AM 1.5G)	-0.6 V	0.39 mA cm ⁻² @ no bias	78.8% Solar-to-hydrogen (STH) efficiency = 0.35%	>1 h	141
	FTO NiO CsPbBr ₃ ZnO Ag FM Pt	0.2 M Na ₂ HPO ₄ /NaH ₂ PO ₄	100 mW cm ⁻² (AM 1.5G)	1.16 V _{RHE}	1.2 mA cm ⁻² @ 0 V _{RHE}	90%		122
Water reduction	ITO NiO MAPbI ₃ PCBM Ag silver paste Ti, foil Pt	0.5 M H ₂ SO ₄	100 mW cm ⁻² (AM 1.5G)	0.95 V _{RHE}	18 mA cm ⁻² @ 0 V _{RHE}	~100%	12 h	142
	FTO Cs ₂ SnI ₆	0.3 M NaCl	150 mW cm ⁻² (AM 1.5G)	-0.15 V _{Hg/Hg₂Cl₂}	0.92 mA cm ⁻² @ -0.8 V _{Hg/Hg₂Cl₂}	Energy conversion efficiency = 0.54%	N/A	143
	APTPE/IrOx (tandem junction)	0.5 M H ₂ SO ₄	100 mW cm ⁻² (AM 1.5G)	2.1 V _{RHE}	12.5 mA cm ⁻² @ 0 V _{RHE}	STH efficiency = 15%	120 h	128

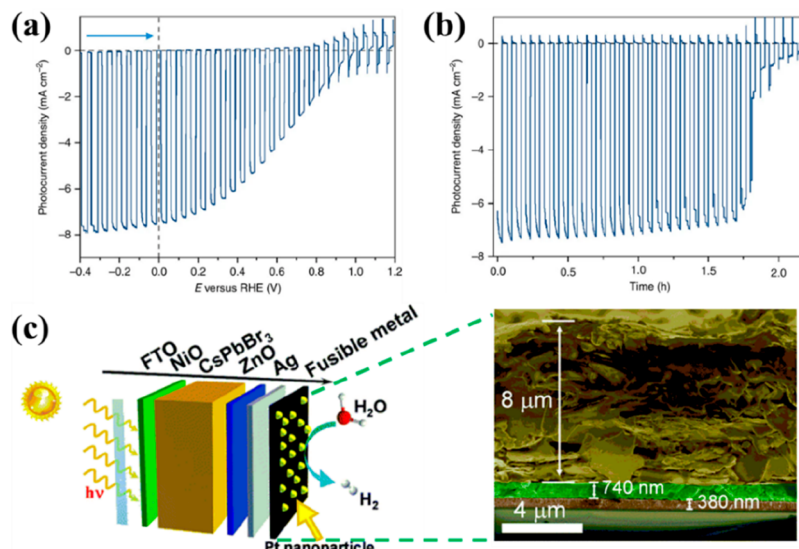


Figure 4. (a) Photocurrent density vs applied bias graph of the MAPbI₃-based photocathode. (b) Photocurrent density vs time graph recorded at 0 V_{RHE}. Reproduced with permission from ref 121. Copyright 2016 Nature. (c) Schematic structure and the cross-sectional SEM image of the CsPbBr₃-based photocathode. Reproduced with permission from ref 141. Copyright 2018 Royal Society of Chemistry.

any protective layers for water oxidation, showing extremely high stability against high temperature and extremely acidic and basic electrolytes (pH = 11). A moderate photocurrent density of 0.8 mA cm⁻² was obtained at 1.23 V_{RHE} (100 mW cm⁻²) with continuous operation for more than 12 h. In addition, Peng and co-workers¹³⁷ synthesized ligand-free Cs₂PtBr₆ NCs, with a corresponding band gap of 1.32 eV with excellent conductivity, which are highly stable against high temperature, moisture and light radiation; the photoelectrodes based on Cs₂PtBr₆ NCs in PEC tests achieved a maximum photocurrent density of 335 μA cm⁻² at -0.6 V_{Ag/AgCl} under LED light (10.18 mW cm⁻²), dramatically outperforming PEC systems based on CsPbBr₃ NCs and Cs₂PdBr₆ NCs (see comparison of photocurrent densities in Figure 3f). More recently, lead-free double perovskite nanocrystals, i.e., Cs₄CuSb₂C₁₂ NCs,¹³⁸ also showed promising photoelectrochemical performance, due to the nature of the direct band gap together with the lower effective mass, which was realized by transforming bulk Cs₄CuSb₂C₁₂ crystals into nanocrystals. We summarize the halide perovskite-based photoanodes in terms of water oxidation performance in Table 1. As it can be noticed, both photoanode- and photocathode-based halide perovskites can reach and even overcome the value of 10 mA/cm², which has been assumed as a break-even point for a given investment.¹³⁹

3.2.2. Halide Perovskite-Based Photocathodes for Hydrogen Evolution. In a PEC system based on a halide perovskite, the p-i-n configuration aims to reduce water through the inverse principle of the n-i-p structure, which transports photogenerated electrons from the perovskite layer to the surface electrode via an ETL such as a PCBM or C₆₀. Similar to the photoanode, FM is widely used as an effective protective layer to protect the perovskite photocathode. As the first example, Quesada and co-workers¹²¹ placed Pt nanoparticles as electrocatalysts on a MAPbI₃-based photocathode, achieving a relatively high current density of 9.8 mA cm⁻² at 0 V_{RHE} and E_{onset} of 0.95 V (Figure 4a,b). The Pt-coated perovskite photocathode showed high stability with 80% retention of its initial photocurrent for about 1 h under constant simulated sunlight (AM = 1.5 G). Later in 2018, the same group¹⁴⁴ used

a state-of-the-art photocathode based on a triple cation halide perovskite (CsFAMA) with a BiVO₄|TiCo photoanode to fabricate a tandem PEC system. The prepared tandem PEC cell with a large area of 10 cm² was able to operate continuously for almost 20 h with an STH efficiency of 0.35% and a small decrease in photocurrent density. Gao and co-workers¹⁴¹ used Pt nanoparticles as FM to fabricate a fully inorganic photocathode based on CsPbBr₃ perovskite, using metal oxides as charge transport layers, i.e., NiO for the HTL and ZnO for the ETL (see PEC cell structure in Figure 4c). The fully inorganic perovskite photocathode achieved a photocurrent density of 1.2 mA cm⁻² at 0 V_{RHE}, and it can maintain ~94% activity after 1 h of continuous illumination.

In addition to the heavily used FM, a low-cost Ti film has been recognized as another type of attractive protective material with high conductivity and photochemical stability. Zhang and co-workers¹²² demonstrated a scalable method to fabricate a sandwich-type photocathode based on MAPbI₃ coated with Ti film, exhibiting an E_{onset} of 0.95 V_{RHE} with an excellent photocurrent density of 18 mA cm⁻² at 0 V_{RHE} in an H₂SO₄-based electrolyte under irradiation of 1 sun. The Ti film-protected photocathode showed high stability after 12 h of continuous light irradiation in aqueous solution (pH: 7–13.6). Regarding the use of lead-free halide perovskites in the production of photocathodes, Dang and co-workers¹⁴² synthesized a Cs₂SnI₆ (Sn⁴⁺) thin film with a high thermal stable phase instead of the widely known yet highly unstable CsSnI₃ (Sn²⁺)¹⁴³ under ambient conditions. The Cs₂SnI₆ photocathode achieved a moderate photocurrent density of 0.92 mA cm⁻² and an energy conversion efficiency of 0.54% at -0.8 V Hg/Hg₂C₁₂ in a NaCl solution, which was attributed to the dense domain of the active sites as well as the slow relaxation dynamics in the excited state through the in-band channel. In order to show a correlation between structure and electronic properties of perovskite photoanodes and halide perovskite-based photocathodes, a comparison of their performance in terms of hydrogen evolution efficiency is also summarized in Table 1.

3.3. Halide Perovskite Electrodes for CO₂ Reduction. The activation of a CO₂ molecule into a CO₂⁻ intermediate

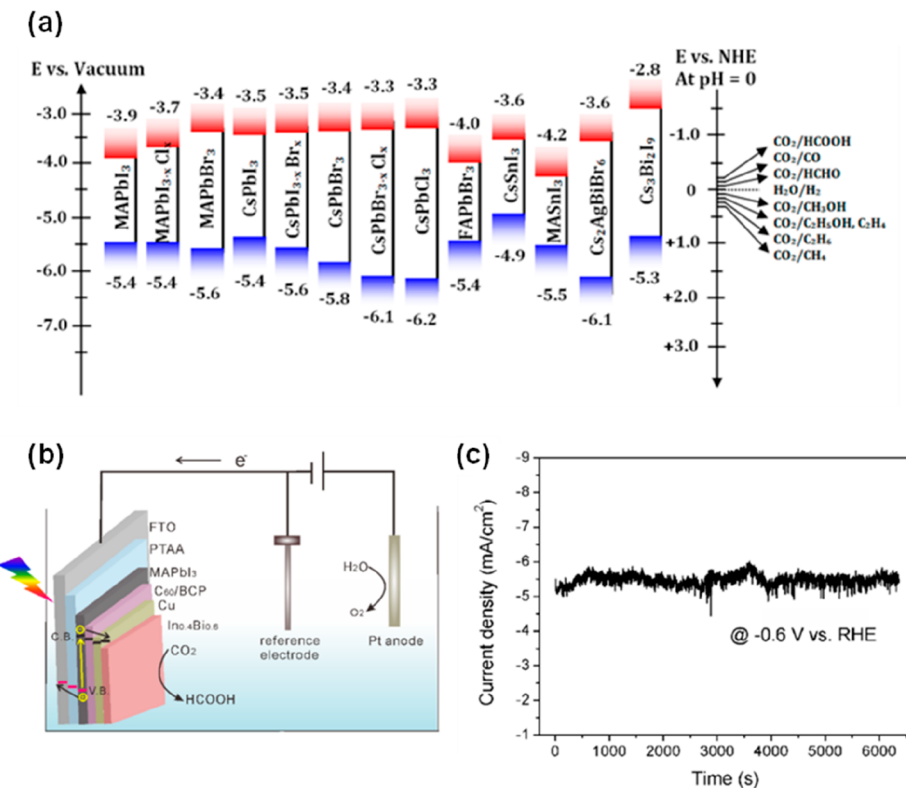


Figure 5. (a) CB and VB positions of various halide perovskite compositions, with respect to both vacuum and NHE levels. The CO₂ redox levels are also present. Reproduced with permission from ref 21. Copyright 2020 American Chemical Society. (b) PEC setup of the In_{0.4}Bi_{0.6}-coated halide perovskite photocathode in a standard three-electrode system. The photocathode is illuminated from the FTO side. The direction of electron or hole flow in the cell is shown. (c) Stability test of the perovskite/In_{0.4}Bi_{0.6} photocathode under 1 sun illumination at -0.6 V vs RHE. Reproduced with permission from ref 150. Copyright 2019 American Chemical Society.

Table 2. Electrochemical Reactions Involved in the Reduction of CO₂ with Water^a

Equation	Product	E ⁰ (V)	E ⁰ (V) vs RHE
CO ₂ + e ⁻ → CO ₂ ⁻	Carbonate anion radical	-1.90	-1.492
CO ₂ + 2H ⁺ + 2e ⁻ → HCOOH	Formic acid	-0.61	-0.202
CO ₂ + 2H ⁺ + 2e ⁻ → CO + H ₂ O	Carbon monoxide	-0.53	-0.122
CO ₂ + 4H ⁺ + 4e ⁻ → HCHO + H ₂ O	Form aldehyde	-0.48	-0.072
CO ₂ + 6H ⁺ + 6e ⁻ → CH ₃ OH + H ₂ O	Methanol	-0.38	0.028
CO ₂ + 8H ⁺ + 8e ⁻ → CH ₄ + 2H ₂ O	Methane	-0.24	0.168

^aTheir corresponding reduction potential (E⁰) (V vs NHE at pH 7) values are also provided. In addition, the equivalent E⁰ (V) vs RHE values are presented.

requires an energy of -1.9 V vs NHE in a neutral pH medium.¹⁴⁵ The reduction of CO₂ by most halide perovskites is a thermodynamically feasible reaction because their conduction bands (CBs) are at relatively higher positions (more negative CBs) than -1.9 V vs NHE, as shown in Figure 5a.²¹ Also, halide perovskites have band gaps higher than 1.34 eV, which is more than the Gibbs free energy (259 kJ mol⁻¹) of the reduction reaction of CO₂ to CO.²² However, a strong negative potential (-1.9 V) is necessary to overcome the energy barrier for the conversion of linear molecule O=C=O into CO₂⁻, which is the rate-determining step for the reactions. Then the CO₂⁻intermediate reacts with protons in aqueous media to form the desired product.¹⁴⁶ The photo-catalytic reduction of CO₂ in aqueous media results in the formation of various products such as formic acid, form-aldehyde, CO, methane (Table 2) and other C₂-C₃ hydrocarbons. Photoreduction of CO₂ by halide perovskites have been studied using both particulate catalysts in

suspension or photoelectrochemical cells^{23,147,148} or deposited ; CO₂ reduction by halide perovskites in the form of a photocathode has rarely been studied. A standard photo-electrochemical cell (PEC) consists of three electrodes; i.e., a reference electrode, a working photoelectrode, and a counter electrode are used for this purpose (Figure 5b).

The working photocathode in the cell structure consists of a halide perovskite layer deposited by spin-coating or other printing methods,¹⁴⁹ an electron transport layer and a conductive electrocatalytic layer (Figure 4c and 5b). These three layers are deposited sequentially on a conductive substrate such as FTO. When the cell is illuminated, the photoexcited electrons of the semiconducting perovskite layer participate in the CO₂ reduction reaction while the holes (photogenerated) are used in the oxidation reaction. The first demonstration of a halide perovskite-based photocathode for CO₂ reduction came from Bakr et al.¹⁵⁰ A photocathode made of MAPbI₃, protected by a conductive In_{0.4}Bi_{0.6} layer, (Figure

Table 3. Summary of Performance of Halide Perovskite-Based PEC Cells toward CO₂ Reduction Reaction

PEC cell configuration	Electrolyte	Irradiation	Onset potential	Photocurrent density	Faradic efficiency	Duration	Ref.
FTO PTAA MAPbI ₃ C60/BCP Cu In _{0.4} Bi _{0.6}	0.1 M KHCO ₃	AM 1.5G	-0.15 V _{RHE}	5.5 mA cm ⁻² @ -0.6 V _{RHE}	~100%	≥1.5 h	150
FTO NiO (Cs _{0.15} FA _{0.85})Pb(I _{0.9} Br _{0.1}) ₃ /CoPc/CNT-C PCBM BCP Au	0.5 M KHCO ₃	100 mW cm ⁻² (AM 1.5G)	0.58 V _{RHE}	15.5 mA cm ⁻² @ -0.11 V _{RHE}	88%	≥25 h	151
FTO NiO _x (CsFAMA)Pb(Br-I) ₃ PCBM PEIE Ag FM Ag epoxyl CoMTPP@CNT	0.5 M KHCO ₃	100 mW cm ⁻² (AM 1.5G)	-0.2 V _{RHE}	5.61 ± 2.90 mA cm ⁻² @ 0 V _{RHE}	N/A	23 h	152
PET ITO PEDOT:PSS PTAA:F4TCNQ (CsFAMA)Pb(Br-I) ₃ PCBM PEIE Ag GE CoMTPP@CNT	0.5 M KHCO ₃	100 mW cm ⁻² (AM 1.5G)	N/A	~7 mA cm ⁻² @ 0 V _{RHE}	N/A	35 h	147
ITO NiO _x BiOI ZnO Cr Ag GE Cu ₉₂ In ₈	0.5 M KHCO ₃	AM 1.5G	N/A	~4–5 mA cm ⁻² @ 0 V _{RHE}	~85%	~24 h	148

Sb) selectively reduced CO₂ to formic acid, which is a commercial chemical compound and hydrogen carrier in fuel cells. In_{0.4}Bi_{0.6} was found to be the best HCOOH-selective electrocatalyst among the In–Bi–Sn three-component alloying systems investigated. In addition to lower electron transfer resistance (as found by electrochemical impedance spectroscopy) and acting as a protective layer for the MAPbI₃ photocathode, the In_{0.4}Bi_{0.6} coating layer stabilizes the HCOO* intermediate in CO₂–HCOOH reaction more than other alloys. This leads to HCOOH production with 100% Faraday efficiency (FE) at a low applied potential of -0.52 V (vs RHE) under 1-sun illumination.¹⁵⁰ The device produced stable current density of 5 mA/cm² for at least 1.5 h monitored at -0.6 V (vs RHE) (Figure 5c).

Subsequently, Zhang et al. used a carbon encapsulation strategy to provide a water-resistant photocathode (Cs_{0.15}FA_{0.85})Pb(I_{0.9}Br_{0.1})₃ toward efficient and stable CO₂ reduction to CO.¹⁵¹ The low-cost carbon layer enabled efficient electron transfer (photogenerated) from the perovskite layer for efficient CO₂ reduction. Perovskite photocathode coated with a molecular cobalt phthalocyanine catalyst layer exhibited a remarkable current density of 15.5 mA cm⁻² under an AM illumination of 1.5G (100 mW cm⁻²), and the photocathode remains stable during the continuous reaction over 25 h, which signifies the state-of-the-art performance of halide perovskite-based photocathodes. They also demonstrated that a tandem cell obtained by combining a carbon-coated perovskite photocathode with a Si-based amorphous photocathode achieved unbiased CO₂ reduction at a photocurrent density of ≈3 mA cm⁻² and an energy conversion efficiency of 3.85%. Andrei et al. also studied unbiased syngas production by a tandem cell consisting of a perovskite-based photocathode and a BiVO₄-based photoanode;¹⁵² a cobalt-based porphyrin catalyst immobilized on CNTs is attached to the tip of the perovskite photocathode. At a low light intensity of 0.1 sun, the photocathode selectively reduces the CO₂ in an aqueous environment for 23 h. The tandem device realizes the conversion of solar energy to CO with an efficiency of 0.02%, suggesting that the device can function as an independent artificial leaf in pH-neutral solutions.¹⁵² In another report, Andrei et al. achieved a CO₂ to CO conversion with solar-to-fuel efficiency of 0.053% using perovskite/BiVO₄-based PEC devices.¹⁴⁷ Furthermore, photocathodes made of BiOI and BiOI–BiVO₄ tandem devices have been successfully run for several hundred hours for syngas production by CO₂ reduction.¹⁴⁸ These design guidelines pave the way for enhancing the efficiency and durability of lead halide perovskites and their low-toxicity analogues that are sensitive to moisture, particularly in the context of solar fuel generation.

Table 3 summarizes the performance of halide perovskite-based photocathodes for the CO₂ reduction reaction.

4. CHALLENGES AND OPPORTUNITIES FOR PEC APPLICATIONS OF MHPs

In this part, we will briefly discuss the major challenges first and then we summarize the opportunities for the future developments in the field; considering that a significant number of review papers were published on water splitting and CO₂ reduction,^{153–159} we will restrict ourselves with issues associated with halide perovskites applications.

4.1. Major Challenges to Overcome. In addition to the common challenges faced in PEC water splitting and the CO₂ reduction process that are summarized in Section 2 and extensively presented elsewhere,^{160,161} we should also overcome two additional challenges if the MHPs will be effectively employed in water splitting or photocatalytic CO₂ reduction: toxicity of their key component (i.e., lead, Pb) and the inherent poor environmental stability (in particular, toward moisture) due to their soft ionic structures. As we discussed in Section 3.1 in detail, a significant amount of effort has been devoted to find an alternative material to substitute Pb; low-toxic alternatives such as divalent metal cations such as Ge²⁺ and Sn²⁺, Sb³⁺ and Bi³⁺ with the electron structures similar to Pb²⁺ have been investigated extensively. The perovskite-like structures obtained by these materials have been mostly tested in photovoltaic devices and often suffered from low efficiency and stability; the same problems may be encountered in PEC applications as well. Nevertheless, the progress is remarkable in the field in terms of both material and device optimization, particularly for Sn²⁺-based perovskites. All these efforts are usually coupled with the efforts to improve the stability of MHPs toward environmental factors, especially against water. The community is still largely focused on developing next-generation Pb-free absorbers for applications in optoelectronics, as well as photocatalysis.

However, the instability of halide perovskites is still the major challenge for their use in photocatalytic and photoelectrochemical applications, even though significant progress has been made in this direction. These materials show poor stability when exposed to air, UV light, high temperature, and water. Charge mobility and high particle diffusivity can also cause instability along the crystal structure. These materials are very sensitive to UV radiation, especially in the presence of air; photodegradation begins when oxygen interacts with the perovskite under illumination.¹⁶² Undesired ion migrations and phase transitions due to thermal degradation can also weaken the crystal structure;¹⁶² exposure to high temperature mainly affects organic cations of perovskites and induces irreversible decomposition.¹⁶³ Among all external stress factors,

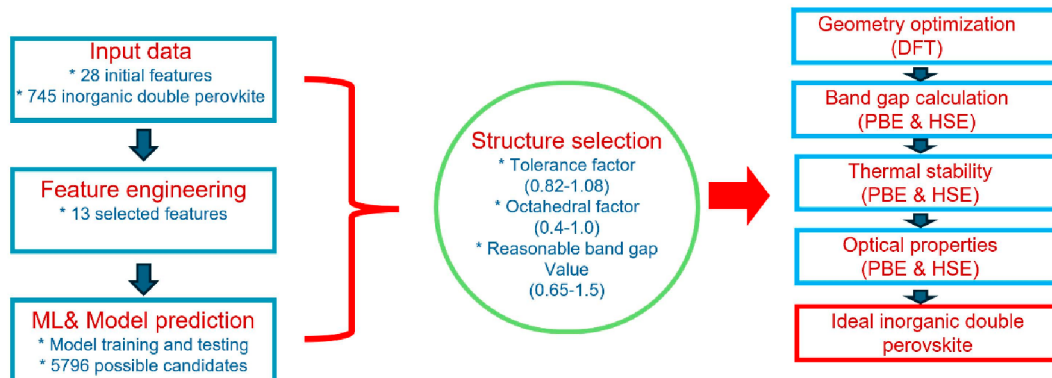


Figure 6. Screening flowchart employed by Gao et al. for lead-free inorganic double perovskites. Adopted from ref 196. Copyright 2021 Elsevier.

water is the most important cause of instability in halide perovskites due to the hygroscopic nature of amine salts, which are organic cations of perovskites.¹⁶⁴ Damage to the crystal structure of the perovskite film results in the loss of optical and electrical properties; it also causes the release of toxic Pb to the environment. Therefore, as a first step, the chemical and structural stability of halide perovskites must be improved if they are to be used in PEC applications.¹²⁰ Indeed numerous strategies have been developed to enhance stability, such as compositional engineering, 2D/3D perovskite structures, surface passivation, protective layers, and encapsulation.^{162,165}

Previous studies on perovskite solar cells indicated that perovskite with mixed cations (MA, FA and Cs) showed higher stability due to uniform grain formation.¹⁶⁴ Perovskites with mixed cations have also been used as a photoelectric active layer for PEC devices with an additional protective effect (discussed below) against direct contact with water.^{152,166,167} In addition, 2D/3D perovskites have been reported as promising candidates for highly stable solar cells; the 2D part of the perovskite layer enhanced stability while the 3D part maintained sufficiently high photoconversion efficiency.¹⁶⁸ However, as far as PEC cells are concerned, dimensional modifications alone have not been sufficient to cope with water diffusion, despite the improvements in the crystal structure of perovskites.^{130,133} Another approach to achieving a highly stable structure is to fabricate monocrystalline perovskites. Single-crystalline perovskites are free of grain boundaries, have a low trap density, and high carrier mobility;¹⁶⁹ hence, solar cells made from perovskite monocrystals usually show excellent stability in humid air.¹⁷⁰ Nevertheless, a photocathode based on perovskite monocrystals also could not resist for long time during water splitting reactions.¹⁷¹ Surface passivation has also been used to improve the optoelectronic properties as well as the stability of halide perovskites. Ionic defects, organic cations, and insufficiently coordinated halide anions, on the surface of perovskites act as trap sites and cause faster degradation.^{172,173} Supramolecular passivating agents have been introduced to control these defect;¹¹⁷ molecules with Lewis acid (electron acceptor) and Lewis base (electron donor) features can successfully attach on the perovskite surface and form halogen bonds, which help to reduce charge-trapping sites, improve the crystallinity of the perovskite, and thus increase stability.^{29,172–174} Even all these strategies are going to improve the intrinsic stability of MHPs, the use of better encapsulates like graphite-epoxy paste¹⁴⁸ or other protection methods against moisture may be still needed.

4.2. Opportunities for Improvement. Remarkable improvements in the light harvesting efficiencies and stability of halide perovskites have been achieved so far in photovoltaic research. The power conversion efficiency has increased from 1% to over 26%¹⁷⁵ while stability has improved from few hours to thousand hours of operation¹⁷⁶ in a bit more than a decade. This trend is likely to continue in the near future because the MHP-based photovoltaics is closer to practical applications. Clearly, most of the desired properties of MHPs and challenges that should be addressed (like light harvesting efficiency, toxicity, and instability) are the same for both photovoltaics and PEC applications; any developments in one field will be beneficial for the other. This is also evident from the fact that there is about a decade time lag between the popularity of MHPs in photovoltaics and PEC applications; some improvements to overcome the inherent weaknesses of MHPs had to be achieved before their use in PEC applications. It is very likely that some portion of the future developments will also be from photovoltaic research. Consequently, one needs to monitor the developments in photovoltaics closely while trying to improve the use of MHP-like materials in PEC applications.

Astonishing developments of computational tools and infrastructure, including efficient ML algorithms, have been combined with the increasing availability of scientific data in materials databases, data repositories, and online journals as well as other computational tools like DFT, and have created an attractive avenue for the discovery of new materials including MHPs. Various ML works on screening different materials (other than halide perovskites) for photocatalytic and PEC water splitting have already appeared in the literature in recent years^{177,178} while only a few cases were involved MHPs.^{179,180} On the other hand, a significant number of a ML work covering various aspects of MHPs in photovoltaics have already been published.^{164,168,181–185} Significant portion of the published work in this field aims to screen DFT generated data for the discovery of thermodynamically stable material with proper band gap; such an approach is usually called high-throughput computational screening. Databases such as International Crystal Structure Database (ICSD),¹⁸⁶ Materials Project (MP),¹⁸⁷ Open Quantum Materials Database (OQMD),¹⁸⁸ Atomic-FLOW for materials discovery (AFLOW),¹⁸⁹ and NOMAD¹⁹⁰ together with high throughput workflow management programs like Firework,¹⁹¹ Atomate,¹⁹² and pymatgen¹⁹³ have been used extensively in recent years. Stability analysis is usually performed, as a first step, directly on data taken from other sources or generated using DFT (at relatively low cost/low accuracy), even if some ML predictions

have also been made. However, screening for band gap usually involves calculating the band gap for a relatively small fraction of the data using more accurate (and more expensive) DFT methods; then, this part of the data set is used to train a predictive ML model to predict the band gap of remaining perovskite materials.

The choice of features (descriptors or input variables) is very important in the construction of an ML model; they should effectively describe the structure–property relationships. Different sets of descriptors have been used with different ML algorithms, as reported in the literature, to tackle the problem from multiple perspectives. For example, Jao et al.,¹⁹⁴ used an elemental code, which is generated from a pseudopotential through a neural network autoencoder, as descriptors and constructed a boosting gradient model for band gap prediction. They used a data set of 1400 lead-free double halide perovskites, generated by high-throughput DFT simulations. Liang et al.,¹⁹⁵ on the other hand, used a data set containing 469 double halide perovskites with features such as ionization potential (IP), Pauling electronegativity (EN), and atomic number (AN) to predict the stability of new perovskite structures. Similarly, Gao et al.¹⁹⁶ screened 5796 double perovskites and proposed 2 candidates, $\text{Na}_2\text{MgMnI}_6$ and K_2NaInI_6 , for use in photovoltaics; the procedure used is given in Figure 6 as an example. They used gradient boosting regression to develop a predictive model for thermodynamic stability and DFT to calculate the frequency response of 748 double halide perovskites. The descriptors were the electrochemical (such as ionization energy) and geometrical (such as ionic radius) properties of A site, B site, B' site, and X site. The corresponding materials were also filtered according to the tolerance factor T_f between 0.82 and 1.08 and the octahedral factor O_f between 0.4 and 1.0. Compounds containing expensive and toxic materials were then eliminated. Finally, a further selection was applied according to the band gap value between 0.8 and 2.0 eV, and 2 candidates were proposed and analyzed in detail for their stability and optical and electrical properties by DFT and Ab initio molecular dynamics. Such works should also be applicable in the search for halide perovskites for photocatalytic and photoelectrochemical applications, as the performance measures are either the same (such as stability) or involve changes in only the desired value (such as band gap); this is also evident from the increasing number of publications of similar works for photocatalysis. For example, Wang et al.¹⁹⁷ recently used a similar approach to find the most suitable configurations of lead free $\text{A}_3\text{B}_2\text{X}_9$ structures for photocatalytic applications.

High-throughput experimentation (HTE), frequently coupled with ML, is another strategy that may be employed to discover or design new MHPs for photovoltaic applications. This approach is quite similar to the computational procedure described above (as their names are also suggested); it can be employed by itself or after the search space is narrowed by computational screening. Although experimental work is generally costlier and more difficult than computational methods, it is almost always needed as the final step because there is no guarantee that computationally discovered material will work in the physical world. For instance, Burger et al.¹⁹⁸ argued that the materials used as batteries, biomaterials, and catalysts are mixtures of molecular and mesoscale components. Such multilength-scale complexity cannot be fully understood by molecular simulations. They used a mobile robot, driven by a Bayesian search algorithm, to improve photocatalysts for

hydrogen production from water. The robot carried out 688 experiments with ten variables over 8 days, and they identified materials that had six times higher activity than the original formulations. Reviews and perspectives have been also published in recent years covering high throughput experimentation for MHPs in general¹⁹⁹ or specific to photocatalytic applications.²⁰⁰ While the use of ML to analyze the data and refine the next step or batches of experiments in HTE is highly beneficial, the use of automation and robotics in synthesis and characterization is also essential as discussed by Sokol and Andrei, who also assess the common fabrication and characterization techniques used in the field by using some automation criteria.²⁰¹

Such diversity in descriptors, tools, and approaches created a rich experience in the field that can be easily extended into new directions including PEC research. Consequently, we can expect that similar paths will be followed for PEC applications, and related works will appear in the literature with increasing numbers in the near future. As the result of similarities in the desired properties of MHPs in photovoltaics and PEC applications, some of the works already performed for photovoltaics may also be used directly in PEC processes. For instance, the toxicity and stability screening of MHPs, as frequently done for photovoltaics, will be also valid for the PEC applications, while the band gap models will need to be retrained.

5. CONCLUSIONS

Metal halide perovskites, hailed by many as the miracle semiconductor for photovoltaics²⁰² of the past decade, exhibit outstanding optoelectronic properties (e.g., broad absorption covering the entire visible range, a tunable band gap, excellent transport properties) and easy solution chemistry from cheap and abundant precursors. They have recently been identified as ideal solid-state photocatalysts for CO_2 reduction, but most reports refer to photocatalytic molecular systems.²⁴ Only a few perovskite-based examples of photoelectrode thin films and photovoltaic-electrocatalytic systems are known. This deficiency is largely due to the well-known challenges associated with perovskites, such as the toxicity of their key component (i.e., lead, Pb) and the inherent poor environmental stability (and in particular toward moisture) due to their soft ionic structures.

Although the stability of halide perovskites remains one of the major challenges for their widespread use in photocatalytic/photoelectrochemical applications, significant progress has been made in this direction. As discussed above, various approaches have been used, such as the use of more stable components (especially cations) and structures (for example, monocrystalline structure), surface passivation, or encapsulations. We can expect more progress in this field in the near future, because halide perovskites are one of the most extensively investigated materials in recent years thanks to their enormous potential in solar cell applications. The research focus on these materials significantly shifted to stability in recent years after the efficiency improved to an acceptable level, making the stability to be the major bottleneck; this creates a big opportunity for the PEC applications of halide perovskites as well because no material could have attracted that much attention and resources if it was related to only PEC applications.

Experimental works combined with ML/DFT analysis can be the most beneficial approach for the effective use of halide

perovskites in PEC applications. As we briefly reviewed, a significant amount of research has been carried out to develop effective strategies for the stability of halide perovskites. Similarly, various ML works on screening different materials (other than halide perovskites) for photocatalytic and photoelectrochemical water splitting have already appeared in the literature in recent years.^{177,178} Therefore, we expect to see more research covering ML applications for halide perovskites for solar water splitting as well as photocatalytic and photoelectrochemical CO₂ reduction. Water-resistant halide perovskites can provide improved solar conversion efficiency in CO₂ reduction, while DFT/ML can make a significant contribution to finding and understanding these materials. Future of this research field looks promising, especially if we also consider the impact of potential developments in experimental and computational resources, including more efficient ML algorithms and increasing data availability on photocatalytic and photoelectrochemical applications of halide perovskites.

AUTHOR INFORMATION

Corresponding Authors

Renata Solarska — Centre of New Technologies, University of Warsaw, 02-097 Warsaw, Poland;  [orcid.org/0000-0002-4811-1143](#); Email: r.solarska@cent.uw.edu.pl

Paola Vivo — Hybrid Solar Cells, Faculty of Engineering and Natural Sciences, Tampere University, FI-33014 Tampere, Finland;  [orcid.org/0000-0003-2872-6922](#);

Email: paola.vivo@tuni.fi

Ramazan Yıldırım — Chemical Engineering Department, Bogazici University, 34342 Bebek, Istanbul, Turkey;  [orcid.org/0000-0001-5077-5689](#); Email: yildirra@bogazici.edu.tr

Authors

Krzysztof Bienkowski — Centre of New Technologies, University of Warsaw, 02-097 Warsaw, Poland

Linh Trinh — Centre of New Technologies, University of Warsaw, 02-097 Warsaw, Poland;  [orcid.org/0000-0001-9829-5166](#)

Justyna Widera-Kalinowska — Department of Chemistry, Adelphi University, Garden City, New York 11530, United States

Basheer Al-Anesi — Hybrid Solar Cells, Faculty of Engineering and Natural Sciences, Tampere University, FI-33014 Tampere, Finland;  [orcid.org/0000-0001-8347-9309](#)

Maning Liu — Hybrid Solar Cells, Faculty of Engineering and Natural Sciences, Tampere University, FI-33014 Tampere, Finland;  [orcid.org/0000-0001-9875-0966](#)

G. Krishnamurthy Grandhi — Hybrid Solar Cells, Faculty of Engineering and Natural Sciences, Tampere University, FI-33014 Tampere, Finland;  [orcid.org/0000-0001-9986-1000](#)

Burcu Oral — Chemical Engineering Department, Bogazici University, 34342 Bebek, Istanbul, Turkey

Beyza Yilmaz — Chemical Engineering Department, Bogazici University, 34342 Bebek, Istanbul, Turkey;  [orcid.org/0000-0001-5735-3729](#)

Complete contact information is available at:

<https://pubs.acs.org/10.1021/acscatal.3c06040>

Notes

The authors declare no competing financial interest.

ACKNOWLEDGMENTS

P.V. thanks the financial support from the Jane and Aatos Erkko foundation through the SOL-TECH project. This work is part of the Research Council of Finland Flagship Programme, Photonics Research and Innovation (PREIN), decision no. 320165. K.B. acknowledges support from the HERA (Hydrogen Energy Rechargeable Architectures) project granted by the National Centre for Research and Development (NCBR). The work was also supported by the National Science Centre Poland (NCN) within the Sonata Bis project 2017/26/E/ST5/01137 granted to R.S. J.W.K. thanks for the financial support the National Science Foundation NSF IRES (grant no. 2107201). R.Y. thanks the financial support from Boğaziçi University Research Fund through project no. 19950.

REFERENCES

- (1) Nocera, D. G. Solar Fuels and Solar Chemicals Industry. *Acc. Chem. Res.* **2017**, *50* (3), 616–619.
- (2) Shih, C. F.; Zhang, T.; Li, J.; Bai, C. Powering the Future with Liquid Sunshine. *Joule* **2018**, *2* (10), 1925–1949.
- (3) Artz, J.; Müller, T. E.; Thenert, K.; Kleinekorte, J.; Meys, R.; Sternberg, A.; Bardow, A.; Leitner, W. Sustainable Conversion of Carbon Dioxide: An Integrated Review of Catalysis and Life Cycle Assessment. *Chem. Rev.* **2018**, *118* (2), 434–504.
- (4) Wang, Y.; Liu, J.; Wang, Y.; Wang, Y.; Zheng, G. Efficient Solar-Driven Electrocatalytic CO₂ Reduction in a Redox-Medium-Assisted System. *Nat. Commun.* **2018**, *9* (1), 5003.
- (5) Proppe, A. H.; Li, Y. C.; Aspuru-Guzik, A.; Berlinguette, C. P.; Chang, C. J.; Cogdell, R.; Doyle, A. G.; Flick, J.; Gabor, N. M.; van Grondelle, R.; Hammes-Schiffer, S.; Jaffer, S. A.; Kelley, S. O.; Leclerc, M.; Leo, K.; Mallouk, T. E.; Narang, P.; Schlau-Cohen, G. S.; Scholes, G. D.; Vojvodic, A.; Yam, V. W.-W.; Yang, J. Y.; Sargent, E. H. Bioinspiration in Light Harvesting and Catalysis. *Nat. Rev. Mater.* **2020**, *5* (11), 828–846.
- (6) Baum, C. M.; Low, S.; Sovacool, B. K. Between the Sun and Us: Expert Perceptions on the Innovation, Policy, and Deep Uncertainties of Space-Based Solar Geoengineering. *Renew. Sustain. Energy Rev.* **2022**, *158*, No. 112179.
- (7) Zhao, X.-G.; Yang, D.; Ren, J.-C.; Sun, Y.; Xiao, Z.; Zhang, L. Rational Design of Halide Double Perovskites for Optoelectronic Applications. *Joule* **2018**, *2* (9), 1662–1673.
- (8) Kahwagi, R. F.; Thornton, S. T.; Smith, B.; Koleilat, G. I. Dimensionality Engineering of Metal Halide Perovskites. *Front. Optoelectron.* **2020**, *13* (3), 196–224.
- (9) Xiao, Z.; Meng, W.; Wang, J.; Mitzi, D. B.; Yan, Y. Searching for Promising New Perovskite-Based Photovoltaic Absorbers: The Importance of Electronic Dimensionality. *Mater. Horizons* **2017**, *4* (2), 206–216.
- (10) Lian, Z.; Yan, Q.; Lv, Q.; Wang, Y.; Liu, L.; Zhang, L.; Pan, S.; Li, Q.; Wang, L.; Sun, J.-L. High-Performance Planar-Type Photodetector on (100) Facet of MAPbI₃ Single Crystal. *Sci. Rep.* **2015**, *5* (1), No. 16563.
- (11) Jena, A. K.; Kulkarni, A.; Miyasaka, T. Halide Perovskite Photovoltaics: Background, Status, and Future Prospects. *Chem. Rev.* **2019**, *119* (5), 3036–3103.
- (12) Manser, J. S.; Christians, J. A.; Kamat, P. V. Intriguing Optoelectronic Properties of Metal Halide Perovskites. *Chem. Rev.* **2016**, *116* (21), 12956–13008.
- (13) Jeong, J.; Kim, M.; Seo, J.; Lu, H.; Ahlawat, P.; Mishra, A.; Yang, Y.; Hope, M. A.; Eickemeyer, F. T.; Kim, M.; Yoon, Y. J.; Choi, I. W.; Darwich, B. P.; Choi, S. J.; Jo, Y.; Lee, J. H.; Walker, B.; Zakeeruddin, S. M.; Emsley, L.; Rothlisberger, U.; Hagfeldt, A.; Kim, D. S.; Grätzel, M.; Kim, J. Y. Pseudo-Halide Anion Engineering for α -FAPbI₃ Perovskite Solar Cells. *Nature* **2021**, *592* (7854), 381–385.
- (14) Yan, J.; Qiu, W.; Wu, G.; Heremans, P.; Chen, H. Recent Progress in 2D/Quasi-2D Layered Metal Halide Perovskites for Solar Cells. *J. Mater. Chem. A* **2018**, *6* (24), 11063–11077.

- (15) Savory, C. N.; Walsh, A.; Scanlon, D. O. Can Pb-Free Halide Double Perovskites Support High-Efficiency Solar Cells? *ACS Energy Lett.* **2016**, *1* (5), 949–955.
- (16) Xiao, Z.; Song, Z.; Yan, Y. From Lead Halide Perovskites to Lead-Free Metal Halide Perovskites and Perovskite Derivatives. *Adv. Mater.* **2019**, *31* (47), 1803792.
- (17) Noel, N. K.; Stranks, S. D.; Abate, A.; Wehrenfennig, C.; Guarnera, S.; Haghghirad, A.-A.; Sadhanala, A.; Eperon, G. E.; Pathak, S. K.; Johnston, M. B.; Petrozza, A.; Herz, L. M.; Snaith, H. J. Lead-Free Organic–Inorganic Tin Halide Perovskites for Photovoltaic Applications. *Energy Environ. Sci.* **2014**, *7* (9), 3061–3068.
- (18) Vivo, P.; Salunke, J.; Priimagi, A. Hole-Transporting Materials for Printable Perovskite Solar Cells. *Materials (Basel)*. **2017**, *10* (9), 1087.
- (19) Noh, J. H.; Im, S. H.; Heo, J. H.; Mandal, T. N.; Seok, S. Il. Chemical Management for Colorful, Efficient, and Stable Inorganic–Organic Hybrid Nanostructured Solar Cells. *Nano Lett.* **2013**, *13* (4), 1764–1769.
- (20) Tan, K. W.; Moore, D. T.; Saliba, M.; Sai, H.; Estroff, L. A.; Hanrath, T.; Snaith, H. J.; Wiesner, U. Thermally Induced Structural Evolution and Performance of Mesoporous Block Copolymer-Directed Alumina Perovskite Solar Cells. *ACS Nano* **2014**, *8* (5), 4730–4739.
- (21) Shyamal, S.; Pradhan, N. Halide Perovskite Nanocrystal Photocatalysts for CO₂ Reduction: Successes and Challenges. *J. Phys. Chem. Lett.* **2020**, *11* (16), 6921–6934.
- (22) Chen, J.; Dong, C.; Idriss, H.; Mohammed, O. F.; Bakr, O. M. Metal Halide Perovskites for Solar-to-Chemical Fuel Conversion. *Adv. Energy Mater.* **2020**, *10* (13), 1902433.
- (23) Zhang, X.; Tang, R.; Li, F.; Zheng, R.; Huang, J. Tailoring Inorganic Halide Perovskite Photocatalysts toward Carbon Dioxide Reduction. *Sol. RRL* **2022**, *6* (6), 2101058.
- (24) Yuan, J.; Liu, H.; Wang, S.; Li, X. How to Apply Metal Halide Perovskites to Photocatalysis: Challenges and Development. *Nanoscale* **2021**, *13* (23), 10281–10304.
- (25) Wang, X.; He, J.; Chen, X.; Ma, B.; Zhu, M. Metal Halide Perovskites for Photocatalytic CO₂ Reduction: An Overview and Prospects. *Coord. Chem. Rev.* **2023**, *482*, No. 215076.
- (26) Chen, S.; Yin, H.; Liu, P.; Wang, Y.; Zhao, H. Stabilization and Performance Enhancement Strategies for Halide Perovskite Photocatalysts. *Adv. Mater.* **2023**, *35* (6), 1–33.
- (27) Guo, K.; Zhang, L.; Shao, S.; Li, J. Photoelectrochemical and First-Principles Investigation on Halide Perovskite/TiO₂ Film Improved by Dicyano Dye. *Opt. Mater. (Amst.)*. **2020**, *109*, No. 110350.
- (28) Zhang, L.; He, M.; Hu, W.; Ge, H. Machine Learning and First-Principles Insights on Molecularly Modified CH₃NH₃PbI₃ Film in Water. *Appl. Surf. Sci.* **2022**, *593*, No. 153428.
- (29) Zhang, L.; Lin, S. Cossensitization-Based Halide Perovskite in Aqueous Solution: A Photoelectrochemical and First-Principles Investigation. *Mater. Res. Bull.* **2021**, *141*, No. 111358.
- (30) Li, S.; Huang, Y.; Zhang, L. Accelerated Design of Stable Halide Perovskite Heterostructure Film in Hostile Condition via Surface Modifier. *Org. Electron.* **2024**, *124*, No. 106945.
- (31) Song, M.-J.; Jin, J.-H. Synergistic Effect of Photoanode and Photocathode Modified with Oxygenated Multi-Walled Carbon Nanotubes in Dye-Sensitized Solar Cells. *Korean J. Chem. Eng.* **2021**, *38* (10), 2129–2133.
- (32) Zhao, Y.; Hoivik, N.; Wang, K. Recent Advance on Engineering Titanium Dioxide Nanotubes for Photochemical and Photoelectrochemical Water Splitting. *Nano Energy* **2016**, *30*, 728–744.
- (33) Bachmeier, A.; Wang, V. C. C.; Woolerton, T. W.; Bell, S.; Fontecilla-Camps, J. C.; Can, M.; Ragsdale, S. W.; Chaudhary, Y. S.; Armstrong, F. A. How Light-Harvesting Semiconductors Can Alter the Bias of Reversible Electrocatalysts in Favor of H₂ Production and CO₂ Reduction. *J. Am. Chem. Soc.* **2013**, *135* (40), 15026–15032.
- (34) Peleyeju, M. G.; Viljoen, E. L. WO₃-Based Catalysts for Photocatalytic and Photoelectrocatalytic Removal of Organic Pollutants from Water – A Review. *J. Water Process Eng.* **2021**, *40*, No. 101930.
- (35) Murillo-Sierra, J. C.; Hernández-Ramírez, A.; Hinojosa-Reyes, L.; Guzmán-Mar, J. L. A Review on the Development of Visible Light-Responsive WO₃-Based Photocatalysts for Environmental Applications. *Chem. Eng. J. Adv.* **2021**, *S*, No. 100070.
- (36) Bagal, I. V.; Chodankar, N. R.; Hassan, M. A.; Waseem, A.; Johar, M. A.; Kim, D.-H.; Ryu, S.-W. Cu₂O as an Emerging Photocathode for Solar Water Splitting - A Status Review. *Int. J. Hydrogen Energy* **2019**, *44* (39), 21351–21378.
- (37) Zhang, Y.-H.; Liu, M.-M.; Chen, J.-L.; Fang, S.-M.; Zhou, P.-P. Recent Advances in Cu₂O-Based Composites for Photocatalysis: A Review. *Dalt. Trans.* **2021**, *50* (12), 4091–4111.
- (38) Siavash Moakhar, R.; Hosseini-Hosseinabad, S. M.; Masudyan, S.; Seza, A.; Jalali, M.; Fallah-Arani, H.; Dabir, F.; Gholipour, S.; Abdi, Y.; Bagheri-Hariri, M.; Riahi-Noori, N.; Lim, Y.; Hagfeldt, A.; Saliba, M. Photoelectrochemical Water-Splitting Using CuO-Based Electrodes for Hydrogen Production: A Review. *Adv. Mater.* **2021**, *33* (33), No. 2007285.
- (39) A, M.; J, M.; Ashokkumar, M.; Arunachalam, P. A Review on BiVO₄ Photocatalyst: Activity Enhancement Methods for Solar Photocatalytic Applications. *Appl. Catal. A Gen.* **2018**, *555*, 47–74.
- (40) Rather, R. A.; Mehta, A.; Lu, Y.; Valant, M.; Fang, M.; Liu, W. Influence of Exposed Facets, Morphology and Hetero-Interfaces of BiVO₄ on Photocatalytic Water Oxidation: A Review. *Int. J. Hydrogen Energy* **2021**, *46* (42), 21866–21888.
- (41) Farhoosh, S.; Eftekharinia, B.; Tayebi, M.; Lee, B.-K.; Naseri, N. Newly Designed Ternary Hematite-Based Heterojunction for PEC Water Splitting. *Appl. Surf. Sci.* **2021**, *550*, No. 149374.
- (42) Rohilla, J.; Ingole, P. P. Optimizing Hematite Nanostructures for Electrochemical and Photoelectrochemical Water Splitting Applications. *Curr. Opin. Green Sustain. Chem.* **2021**, *29*, No. 100455.
- (43) Prusty, D.; Paramanik, L.; Parida, K. Recent Advances on Alloyed Quantum Dots for Photocatalytic Hydrogen Evolution: A Mini-Review. *Energy Fuels* **2021**, *35* (6), 4670–4686.
- (44) Abdullah, U.; Ali, M.; Pervaiz, E. An Inclusive Review on Recent Advancements of Cadmium Sulfide Nanostructures and Its Hybrids for Photocatalytic and Electrocatalytic Applications. *Mol. Catal.* **2021**, *508*, No. 111575.
- (45) Yang, K.; Yang, Z.; Zhang, C.; Gu, Y.; Wei, J.; Li, Z.; Ma, C.; Yang, X.; Song, K.; Li, Y.; Fang, Q.; Zhou, J. Recent Advances in CdS-Based Photocatalysts for CO₂ Photocatalytic Conversion. *Chem. Eng. J.* **2021**, *418*, No. 129344.
- (46) Ma, Y.; Zhou, K.; Dong, H.; Zhou, X. Effects of Adsorbing Noble Metal Single Atoms on the Electronic Structure and Photocatalytic Activity of Ta₃N₅. *J. Phys. Chem. C* **2021**, *125* (32), 17600–17611.
- (47) Zhang, M.; Yang, Y.; An, X.; Hou, L. A Critical Review of G-C₃N₄-Based Photocatalytic Membrane for Water Purification. *Chem. Eng. J.* **2021**, *412*, No. 128663.
- (48) Zhu, Q.; Xu, Z.; Qiu, B.; Xing, M.; Zhang, J. Emerging Cocatalysts on G-C₃N₄ for Photocatalytic Hydrogen Evolution. *Small* **2021**, *17* (40), 2101070.
- (49) Ai, L.; Shi, R.; Yang, J.; Zhang, K.; Zhang, T.; Lu, S. Efficient Combination of G-C₃N₄ and CDs for Enhanced Photocatalytic Performance: A Review of Synthesis, Strategies, and Applications. *Small* **2021**, *17* (48), 2007523.
- (50) Ran, J.; Zhang, J.; Yu, J.; Jaroniec, M.; Qiao, S. Z. Earth-Abundant Cocatalysts for Semiconductor-Based Photocatalytic Water Splitting. *Chem. Soc. Rev.* **2014**, *43* (22), 7787–7812.
- (51) Hasija, V.; Kumar, A.; Sudhaik, A.; Raizada, P.; Singh, P.; Van Le, Q.; Le, T. T.; Nguyen, V.-H. Step-Scheme Heterojunction Photocatalysts for Solar Energy, Water Splitting, CO₂ Conversion, and Bacterial Inactivation: A Review. *Environ. Chem. Lett.* **2021**, *19* (4), 2941–2966.
- (52) Blakemore, J. D.; Crabtree, R. H.; Brudvig, G. W. Molecular Catalysts for Water Oxidation. *Chem. Rev.* **2015**, *115* (23), 12974–13005.

- (53) Kotes Kumar, M.; Naresh, G.; Vijay Kumar, V.; Sai Vasista, B.; Sasikumar, B.; Venugopal, A. Improved H₂ Yields over Cu-Ni-TiO₂ under Solar Light Irradiation: Behaviour of Alloy Nano Particles on Photocatalytic H₂O Splitting. *Appl. Catal. B Environ.* **2021**, *299*, No. 120654.
- (54) Zhang, Y.; Zhao, J.; Wang, H.; Xiao, B.; Zhang, W.; Zhao, X.; Lv, T.; Thangamuthu, M.; Zhang, J.; Guo, Y.; Ma, J.; Lin, L.; Tang, J.; Huang, R.; Liu, Q. Single-Atom Cu Anchored Catalysts for Photocatalytic Renewable H₂ Production with a Quantum Efficiency of 56%. *Nat. Commun.* **2022**, *13* (1), 58.
- (55) Wang, C.; Xie, J.; Chen, N.; Chen, W.; Bai, P.; Wang, H. Non-Noble-Metal Catalyst of Cu/g-C₃N₄ for Efficient Photocatalytic Hydrogen Evolution. *ACS Appl. Energy Mater.* **2021**, *4* (12), 13796–13802.
- (56) Esmat, M.; Doustkhah, E.; Abdelbar, M.; Tahawy, R.; El-Hosainy, H.; Abdelhameed, M.; Ide, Y.; Fukata, N. Structural Conversion of Cu-Titanate into Photoactive Plasmonic Cu-TiO₂ for H₂ Generation in Visible Light. *ACS Sustain. Chem. Eng.* **2022**, *10* (13), 4143–4151.
- (57) Kim, D. J.; Tonda, S.; Jo, W.-K. Application of Cu-Loaded One-Dimensional TiO₂ Nanorods for Elevated Photocatalytic Environmental Friendly Hydrogen Production. *J. Environ. Sci. Int.* **2021**, *30* (1), 57–67.
- (58) Kumar, V.; Singh, N.; Jana, S.; Rout, S. K.; Dey, R. K.; Singh, G. P. Surface Polar Charge Induced Ni Loaded CdS Heterostructure Nanorod for Efficient Photo-Catalytic Hydrogen Evolution. *Int. J. Hydrogen Energy* **2021**, *46* (30), 16373–16386.
- (59) Raza, J.; Khoja, A. H.; Naqvi, S. R.; Mehran, M. T.; Shakir, S.; Liaquat, R.; Tahir, M.; Ali, G. Methane Decomposition for Hydrogen Production over Biomass Fly Ash-Based CeO₂ Nanowires Promoted Cobalt Catalyst. *J. Environ. Chem. Eng.* **2021**, *9* (5), No. 105816.
- (60) Ye, T.-N.; Park, S.-W.; Lu, Y.; Li, J.; Wu, J.; Sasase, M.; Kitano, M.; Hosono, H. Dissociative and Associative Concerted Mechanism for Ammonia Synthesis over Co-Based Catalyst. *J. Am. Chem. Soc.* **2021**, *143* (32), 12857–12866.
- (61) Low, J.; Cheng, B.; Yu, J.; Jaroniec, M. Carbon-Based Two-Dimensional Layered Materials for Photocatalytic CO₂ Reduction to Solar Fuels. *Energy Storage Mater.* **2016**, *3*, 24–35.
- (62) Ali, S.; Razzaq, A.; In, S.-I. Development of Graphene Based Photocatalysts for CO₂ Reduction to C₁ Chemicals: A Brief Overview. *Catal. Today* **2019**, *335*, 39–54.
- (63) Sun, Z.; Wang, H.; Wu, Z.; Wang, L. G-C₃N₄ Based Composite Photocatalysts for Photocatalytic CO₂ Reduction. *Catal. Today* **2018**, *300*, 160–172.
- (64) Xie, W.; Xu, J.; Md Idros, U.; Katsuhira, J.; Fuki, M.; Hayashi, M.; Yamanaka, M.; Kobori, Y.; Matsubara, R. Metal-Free Reduction of CO₂ to Formate Using a Photochemical Organohydride-Catalyst Recycling Strategy. *Nat. Chem.* **2023**, *15* (6), 794–802.
- (65) Mesa, C. A.; Francàs, L.; Yang, K. R.; Garrido-Barros, P.; Pastor, E.; Ma, Y.; Kafizas, A.; Rosser, T. E.; Mayer, M. T.; Reisner, E.; Grätzel, M.; Batista, V. S.; Durrant, J. R. Multihole Water Oxidation Catalysis on Haematite Photoanodes Revealed by Operando Spectroelectrochemistry and DFT. *Nat. Chem.* **2020**, *12* (1), 82–89.
- (66) Kalamaras, E.; Maroto-Valer, M. M.; Shao, M.; Xuan, J.; Wang, H. Solar Carbon Fuel via Photoelectrochemistry. *Catal. Today* **2018**, *317*, 56–75.
- (67) Zhao, J.; Wang, X.; Xu, Z.; Loo, J. S. C. Hybrid Catalysts for Photoelectrochemical Reduction of Carbon Dioxide: A Prospective Review on Semiconductor/Metal Complex Co-Catalyst Systems. *J. Mater. Chem. A* **2014**, *2* (37), 15228.
- (68) Pawar, A. U.; Kim, C. W.; Nguyen-Le, M.-T.; Kang, Y. S. General Review on the Components and Parameters of Photoelectrochemical System for CO₂ Reduction with in Situ Analysis. *ACS Sustain. Chem. Eng.* **2019**, *7* (8), 7431–7455.
- (69) Elbersen, R.; Vijselaar, W.; Tiggelaar, R. M.; Gardeniers, H.; Huskens, J. Effects of Pillar Height and Junction Depth on the Performance of Radially Doped Silicon Pillar Arrays for Solar Energy Applications. *Adv. Energy Mater.* **2016**, *6* (3), 1501728.
- (70) Birdja, Y. Y.; Pérez-Gallent, E.; Figueiredo, M. C.; Göttle, A. J.; Calle-Vallejo, F.; Koper, M. T. M. Advances and Challenges in Understanding the Electrocatalytic Conversion of Carbon Dioxide to Fuels. *Nat. Energy* **2019**, *4* (9), 732–745.
- (71) Kibria, M. G.; Edwards, J. P.; Gabardo, C. M.; Dinh, C.; Seifitokaldani, A.; Sinton, D.; Sargent, E. H. Electrochemical CO₂ Reduction into Chemical Feedstocks: From Mechanistic Electrocatalysis Models to System Design. *Adv. Mater.* **2019**, *31* (31), 1807166.
- (72) Han, N.; Ding, P.; He, L.; Li, Y.; Li, Y. Promises of Main Group Metal-Based Nanostructured Materials for Electrochemical CO₂ Reduction to Formate. *Adv. Energy Mater.* **2020**, *10* (11), 1902338.
- (73) Chang, X.; Wang, T.; Yang, P.; Zhang, G.; Gong, J. The Development of Cocatalysts for Photoelectrochemical CO₂ Reduction. *Adv. Mater.* **2019**, *31* (31), 1804710.
- (74) Esswein, A. J.; Surendranath, Y.; Reece, S. Y.; Nocera, D. G. Highly Active Cobalt Phosphate and Borate Based Oxygen Evolving Catalysts Operating in Neutral and Natural Waters. *Energy Environ. Sci.* **2011**, *4* (2), 499–504.
- (75) Møller, C. K. A Phase Transition in Cæsium Plumbochloride. *Nature* **1957**, *180* (4593), 981–982.
- (76) Møller, C. K. Crystal Structure and Photoconductivity of Cæsium Plumbobhalides. *Nature* **1958**, *182* (4647), 1436–1436.
- (77) Weber, D. CH₃NH₃SnBr_xI_{3-x} (x = 0–3), Ein Sn(II)-System Mit Kubischer Perowskitstruktur/CH₃NH₃SnBr_xI_{3-x} (x = 0–3), a Sn(II)-System with Cubic Perovskite Structure. *Zeitschrift für Naturforsch. B* **1978**, *33* (8), 862–865.
- (78) Stranks, S. D.; Eperon, G. E.; Grancini, G.; Menelaou, C.; Alcocer, M. J. P.; Leijtens, T.; Herz, L. M.; Petrozza, A.; Snaith, H. J. Electron-Hole Diffusion Lengths Exceeding 1 Micrometer in an Organometal Trihalide Perovskite Absorber. *Science* (80-.). **2013**, *342* (6156), 341–344.
- (79) Dong, Q.; Fang, Y.; Shao, Y.; Mulligan, P.; Qiu, J.; Cao, L.; Huang, J. Electron-Hole Diffusion Lengths > 175 Mm in Solution-Grown CH₃NH₃PbI₃ Single Crystals. *Science* (80-.). **2015**, *347* (6225), 967–970.
- (80) Kung, P.-K.; Li, M.-H.; Lin, P.-Y.; Jhang, J.-Y.; Pantaler, M.; Lupascu, D. C.; Grancini, G.; Chen, P. Lead-Free Double Perovskites for Perovskite Solar Cells. *Sol. RRL* **2020**, *4* (2), 1–32.
- (81) Kulkarni, S. A.; Baikie, T.; Boix, P. P.; Yantara, N.; Mathews, N.; Mhaisalkar, S. Band-Gap Tuning of Lead Halide Perovskites Using a Sequential Deposition Process. *J. Mater. Chem. A* **2014**, *2* (24), 9221–9225.
- (82) HUANG, F.; SONG, J.; LIAO, P.; WANG, M. The Stability of Perovskite Solar Cells. *Chin. Sci. Bull.* **2017**, *62* (36), 4256–4269.
- (83) Hoye, R. L. Z.; Hidalgo, J.; Jagt, R. A.; Correa-Baena, J.; Fix, T.; MacManus-Driscoll, J. L. The Role of Dimensionality on the Optoelectronic Properties of Oxide and Halide Perovskites, and Their Halide Derivatives. *Adv. Energy Mater.* **2022**, *12* (4), 2100499.
- (84) Trifiletti, V.; Asker, C.; Tseberlidis, G.; Riva, S.; Zhao, K.; Tang, W.; Binetti, S.; Fenwick, O. Quasi-Zero Dimensional Halide Perovskite Derivatives: Synthesis, Status, and Opportunity. *Front. Electron.* **2021**, *2*. DOI: 10.3389/felec.2021.758603.
- (85) Chen, D.; Wan, Z.; Chen, X.; Yuan, Y.; Zhong, J. Large-Scale Room-Temperature Synthesis and Optical Properties of Perovskite-Related Cs₄PbBr₆ Fluorophores. *J. Mater. Chem. C* **2016**, *4* (45), 10646–10653.
- (86) Xiao, Z.; Yan, Y. Progress in Theoretical Study of Metal Halide Perovskite Solar Cell Materials. *Adv. Energy Mater.* **2017**, *7* (22), 1701136.
- (87) Leung, T. L.; Ahmad, I.; Syed, A. A.; Ng, A. M. C.; Popović, J.; Djurišić, A. B. Stability of 2D and Quasi-2D Perovskite Materials and Devices. *Commun. Mater.* **2022**, *3* (1), 63.
- (88) Mahal, E.; Mandal, S. C.; Pathak, B. Understanding the Role of Spacer Cation in 2D Layered Halide Perovskites to Achieve Stable Perovskite Solar Cells. *Mater. Adv.* **2022**, *3* (5), 2464–2474.
- (89) Brgoch, J.; Lehner, A. J.; Chabinyc, M.; Seshadri, R. Ab Initio Calculations of Band Gaps and Absolute Band Positions of Polymorphs of RbPbI₃ and CsPbI₃: Implications for Main-Group

- Halide Perovskite Photovoltaics. *J. Phys. Chem. C* **2014**, *118* (48), 27721–27727.
- (90) Yin, W.; Shi, T.; Yan, Y. Unique Properties of Halide Perovskites as Possible Origins of the Superior Solar Cell Performance. *Adv. Mater.* **2014**, *26* (27), 4653–4658.
- (91) Li, X.; Traoré, B.; Kepenekian, M.; Li, L.; Stoumpos, C. C.; Guo, P.; Even, J.; Katan, C.; Kanatzidis, M. G. Bismuth/Silver-Based Two-Dimensional Iodide Double and One-Dimensional Bi Perovskites: Interplay between Structural and Electronic Dimensions. *Chem. Mater.* **2021**, *33* (15), 6206–6216.
- (92) Lyu, M.; Yun, J.; Chen, P.; Hao, M.; Wang, L. Addressing Toxicity of Lead: Progress and Applications of Low-Toxic Metal Halide Perovskites and Their Derivatives. *Adv. Energy Mater.* **2017**, *7* (15), 1602512.
- (93) Raza, E.; Aziz, F.; Ahmad, Z. Stability of Organometal Halide Perovskite Solar Cells and Role of HTMs: Recent Developments and Future Directions. *RSC Adv.* **2018**, *8* (37), 20952–20967.
- (94) Stoumpos, C. C.; Frazer, L.; Clark, D. J.; Kim, Y. S.; Rhim, S. H.; Freeman, A. J.; Ketterson, J. B.; Jang, J. I.; Kanatzidis, M. G. Hybrid Germanium Iodide Perovskite Semiconductors: Active Lone Pairs, Structural Distortions, Direct and Indirect Energy Gaps, and Strong Nonlinear Optical Properties. *J. Am. Chem. Soc.* **2015**, *137* (21), 6804–6819.
- (95) Chung, I.; Song, J.-H.; Im, J.; Androulakis, J.; Malliakas, C. D.; Li, H.; Freeman, A. J.; Kenney, J. T.; Kanatzidis, M. G. CsSnI₃: Semiconductor or Metal? High Electrical Conductivity and Strong Near-Infrared Photoluminescence from a Single Material. High Hole Mobility and Phase-Transitions. *J. Am. Chem. Soc.* **2012**, *134* (20), 8579–8587.
- (96) Stoumpos, C. C.; Malliakas, C. D.; Kanatzidis, M. G. Semiconducting Tin and Lead Iodide Perovskites with Organic Cations: Phase Transitions, High Mobilities, and Near-Infrared Photoluminescent Properties. *Inorg. Chem.* **2013**, *52* (15), 9019–9038.
- (97) Krishnamoorthy, T.; Ding, H.; Yan, C.; Leong, W. L.; Baikie, T.; Zhang, Z.; Sherburne, M.; Li, S.; Asta, M.; Mathews, N.; Mhaisalkar, S. G. Lead-Free Germanium Iodide Perovskite Materials for Photovoltaic Applications. *J. Mater. Chem. A* **2015**, *3* (47), 23829–23832.
- (98) Konstantakou, M.; Stergiopoulos, T. A Critical Review on Tin Halide Perovskite Solar Cells. *J. Mater. Chem. A* **2017**, *5* (23), 11518–11549.
- (99) Babayigit, A.; Ethirajan, A.; Muller, M.; Conings, B. Toxicity of Organometal Halide Perovskite Solar Cells. *Nat. Mater.* **2016**, *15* (3), 247–251.
- (100) Cheng, J.; Zhang, M.; Wu, G.; Wang, X.; Zhou, J.; Cen, K. Optimizing CO₂ Reduction Conditions to Increase Carbon Atom Conversion Using a Pt-RGO||Pt-TNT Photoelectrochemical Cell. *Sol. Energy Mater. Sol. Cells* **2015**, *132*, 606–614.
- (101) Xu, Z.; Mitzi, D. B.; Dimitrakopoulos, C. D.; Maxcy, K. R. Semiconducting Perovskites (2-XC₆H₄C₂H₄NH₃)₂SnI₄ (X = F, Cl, Br): Steric Interaction between the Organic and Inorganic Layers. *Inorg. Chem.* **2003**, *42* (6), 2031–2039.
- (102) Reddy, S. H.; Sumukam, R. R.; Murali, B. Can Perovskite Inspired Bismuth Halide Nanocrystals Outperform Their Lead Counterparts? *J. Mater. Chem. A* **2020**, *8* (26), 12951–12963.
- (103) Lee, L. C.; Huq, T. N.; MacManus-Driscoll, J. L.; Hoye, R. L. Z. Research Update: Bismuth-Based Perovskite-Inspired Photovoltaic Materials. *APL Mater.* **2018**, *6* (8), No. 084502.
- (104) Turkevych, I.; Kazaoui, S.; Ito, E.; Urano, T.; Yamada, K.; Tomiyasu, H.; Yamagishi, H.; Kondo, M.; Aramaki, S. Photovoltaic Rudorffites: Lead-Free Silver Bismuth Halides Alternative to Hybrid Lead Halide Perovskites. *ChemSusChem* **2017**, *10* (19), 3754–3759.
- (105) Kim, Y.; Yang, Z.; Jain, A.; Voznyy, O.; Kim, G.; Liu, M.; Quan, L. N.; García de Arquer, F. P.; Comin, R.; Fan, J. Z.; Sargent, E. H. Pure Cubic-Phase Hybrid Iodobismuthates AgBi₂I₇ for Thin-Film Photovoltaics. *Angew. Chemie Int. Ed.* **2016**, *55* (33), 9586–9590.
- (106) Ghosh, B.; Wu, B.; Guo, X.; Harikesh, P. C.; John, R. A.; Baikie, T.; Arramel, Wee, A. T. S.; Guet, C.; Sum, T. C.; Mhaisalkar, S.; Mathews, N. Superior Performance of Silver Bismuth Iodide Photovoltaics Fabricated via Dynamic Hot-Casting Method under Ambient Conditions. *Adv. Energy Mater.* **2018**, *8* (33), 1802051.
- (107) Sansom, H. C.; Whitehead, G. F. S.; Dyer, M. S.; Zanella, M.; Manning, T. D.; Pitcher, M. J.; Whittles, T. J.; Dhanak, V. R.; Alaria, J.; Claridge, J. B.; Rosseinsky, M. J. AgBiI₄ as a Lead-Free Solar Absorber with Potential Application in Photovoltaics. *Chem. Mater.* **2017**, *29* (4), 1538–1549.
- (108) Park, B.; Philippe, B.; Zhang, X.; Rensmo, H.; Boschloo, G.; Johansson, E. M. J. Bismuth Based Hybrid Perovskites A₃Bi₂I₉ (A: Methylammonium or Cesium) for Solar Cell Application. *Adv. Mater.* **2015**, *27* (43), 6806–6813.
- (109) Saparov, B.; Hong, F.; Sun, J.-P.; Duan, H.-S.; Meng, W.; Cameron, S.; Hill, I. G.; Yan, Y.; Mitzi, D. B. Thin-Film Preparation and Characterization of Cs₃Sb₂I₉: A Lead-Free Layered Perovskite Semiconductor. *Chem. Mater.* **2015**, *27* (16), 5622–5632.
- (110) Singh, A.; Boopathi, K. M.; Mohapatra, A.; Chen, Y. F.; Li, G.; Chu, C. W. Photovoltaic Performance of Vapor-Assisted Solution-Processed Layer Polymorph of Cs₃Sb₂I₉. *ACS Appl. Mater. Interfaces* **2018**, *10* (3), 2566–2573.
- (111) Huang, Y.-T.; Kavanagh, S. R.; Scanlon, D. O.; Walsh, A.; Hoye, R. L. Z. Perovskite-Inspired Materials for Photovoltaics and beyond—from Design to Devices. *Nanotechnology* **2021**, *32* (13), 132004.
- (112) Zhou, J.; Huang, J. Photodetectors Based on Organic–Inorganic Hybrid Lead Halide Perovskites. *Adv. Sci.* **2018**, *5* (1). DOI: [10.1002/advs.201700256](https://doi.org/10.1002/advs.201700256).
- (113) Slavney, A. H.; Hu, T.; Lindenberg, A. M.; Karunadasa, H. I. A Bismuth-Halide Double Perovskite with Long Carrier Recombination Lifetime for Photovoltaic Applications. *J. Am. Chem. Soc.* **2016**, *138* (7), 2138–2141.
- (114) Soultati, A.; Tountas, M.; Armadorou, K. K.; Yusoff, A. R. b. M.; Vasilopoulou, M.; Nazeeruddin, M. K. Synthetic Approaches for Perovskite Thin Films and Single-Crystals. *Energy Adv.* **2023**, *2* (8), 1075–1115.
- (115) Shamsi, J.; Urban, A. S.; Imran, M.; De Trizio, L.; Manna, L. Metal Halide Perovskite Nanocrystals: Synthesis, Post-Synthesis Modifications, and Their Optical Properties. *Chem. Rev.* **2019**, *119* (5), 3296–3348.
- (116) Huang, Y.; Yu, J.; Wu, Z.; Li, B.; Li, M. All-Inorganic Lead Halide Perovskites for Photocatalysis: A Review. *RSC Adv.* **2024**, *14* (7), 4946–4965.
- (117) Canil, L.; Salunke, J.; Wang, Q.; Liu, M.; Köbler, H.; Flatken, M.; Gregori, L.; Meggiolaro, D.; Ricciarelli, D.; De Angelis, F.; Stolterfoht, M.; Neher, D.; Priimagi, A.; Vivo, P.; Abate, A. Halogen-Bonded Hole-Transport Material Suppresses Charge Recombination and Enhances Stability of Perovskite Solar Cells. *Adv. Energy Mater.* **2021**, *11* (35). DOI: [10.1002/aenm.202101553](https://doi.org/10.1002/aenm.202101553).
- (118) Wang, N.; Cheng, L.; Ge, R.; Zhang, S.; Miao, Y.; Zou, W.; Yi, C.; Sun, Y.; Cao, Y.; Yang, R.; Wei, Y.; Guo, Q.; Ke, Y.; Yu, M.; Jin, Y.; Liu, Y.; Ding, Q.; Di, D.; Yang, L.; Xing, G.; Tian, H.; Jin, C.; Gao, F.; Friend, R. H.; Wang, J.; Huang, W. Perovskite Light-Emitting Diodes Based on Solution-Processed Self-Organized Multiple Quantum Wells. *Nat. Photonics* **2016**, *10* (11), 699–704.
- (119) Mei, J.; Liu, M.; Vivo, P.; Pecunia, V. Two-Dimensional Antimony-Based Perovskite-Inspired Materials for High-Performance Self-Powered Photodetectors. *Adv. Funct. Mater.* **2021**, *31* (50), 2106295.
- (120) Singh, S.; Chen, H.; Shahrokhi, S.; Wang, L. P.; Lin, C.-H.; Hu, L.; Guan, X.; Tricoli, A.; Xu, Z. J.; Wu, T. Hybrid Organic–Inorganic Materials and Composites for Photoelectrochemical Water Splitting. *ACS Energy Lett.* **2020**, *5* (5), 1487–1497.
- (121) Crespo-Quesada, M.; Pazos-Outón, L. M.; Warnan, J.; Kuehnel, M. F.; Friend, R. H.; Reisner, E. Metal-Encapsulated Organolead Halide Perovskite Photocathode for Solar-Driven Hydrogen Evolution in Water. *Nat. Commun.* **2016**, *7* (1), 12555.

- (122) Zhang, H.; Yang, Z.; Yu, W.; Wang, H.; Ma, W.; Zong, X.; Li, C. A Sandwich-Like Organolead Halide Perovskite Photocathode for Efficient and Durable Photoelectrochemical Hydrogen Evolution in Water. *Adv. Energy Mater.* **2018**, *8* (22), 1–7.
- (123) Pornrungroj, C.; Andrei, V.; Rahaman, M.; Uswachoke, C.; Joyce, H. J.; Wright, D. S.; Reisner, E. Bifunctional Perovskite-BiVO₄ Tandem Devices for Uninterrupted Solar and Electrocatalytic Water Splitting Cycles. *Adv. Funct. Mater.* **2021**, *31* (15), 1–9.
- (124) Choi, H.; Seo, S.; Yoon, C. J.; Ahn, J.; Kim, C.; Jung, Y.; Kim, Y.; Toma, F. M.; Kim, H.; Lee, S. Organometal Halide Perovskite-Based Photoelectrochemical Module Systems for Scalable Unassisted Solar Water Splitting. *Adv. Sci.* **2023**, *10* (33), 1–12.
- (125) Yun, J.; Lee, H.; Park, Y. S.; Jeong, W.; Jeong, C.; Lee, J.; Lee, J.; Tan, J.; Ma, S.; Jang, G.; Lee, C. U.; Moon, S.; Im, H.; Lee, S.; Yee, D.; Kim, J.; Moon, J. Conductive Passivator and Dipole Layer Mixture Enabling High-Performance Stable Perovskite Photoelectrode-Based Solar Water Splitting. *Adv. Energy Mater.* **2023**, *13* (46), 1–13.
- (126) Rhee, R.; Kim, T. G.; Jang, G. Y.; Bae, G.; Lee, J. H.; Lee, S.; Kim, S.; Jeon, S.; Park, J. H. Unassisted Overall Water Splitting with a Solar-to-hydrogen Efficiency of over 10% by Coupled Lead Halide Perovskite Photoelectrodes. *Carbon Energy* **2023**, *5* (1), 1–10.
- (127) Fehr, A. M. K.; Agrawal, A.; Mandani, F.; Conrad, C. L.; Jiang, Q.; Park, S. Y.; Alley, O.; Li, B.; Sidhik, S.; Metcalf, I.; Botello, C.; Young, J. L.; Even, J.; Blancon, J. C.; Deutsch, T. G.; Zhu, K.; Albrecht, S.; Toma, F. M.; Wong, M.; Mohite, A. D. Integrated Halide Perovskite Photoelectrochemical Cells with Solar-Driven Water-Splitting Efficiency of 20.8%. *Nat. Commun.* **2023**, *14* (1), 3797.
- (128) Song, Z.; Li, C.; Chen, L.; Dolia, K.; Fu, S.; Sun, N.; Li, Y.; Wyatt, K.; Young, J. L.; Deutsch, T. G.; Yan, Y. All-Perovskite Tandem Photoelectrodes for Unassisted Solar Hydrogen Production. *ACS Energy Lett.* **2023**, *8* (6), 2611–2619.
- (129) Da, P.; Cha, M.; Sun, L.; Wu, Y.; Wang, Z.-S.; Zheng, G. High-Performance Perovskite Photoanode Enabled by Ni Passivation and Catalysis. *Nano Lett.* **2015**, *15* (5), 3452–3457.
- (130) Wang, C.; Yang, S.; Chen, X.; Wen, T.; Yang, H. G. Surface-Functionalized Perovskite Films for Stable Photoelectrochemical Water Splitting. *J. Mater. Chem. A* **2017**, *5* (3), 910–913.
- (131) Hoang, M. T.; Pham, N. D.; Han, J. H.; Gardner, J. M.; Oh, I. Integrated Photoelectrolysis of Water Implemented On Organic Metal Halide Perovskite Photoelectrode. *ACS Appl. Mater. Interfaces* **2016**, *8* (19), 11904–11909.
- (132) Nam, S.; Mai, C. T. K.; Oh, I. Ultrastable Photoelectrodes for Solar Water Splitting Based on Organic Metal Halide Perovskite Fabricated by Lift-Off Process. *ACS Appl. Mater. Interfaces* **2018**, *10* (17), 14659–14664.
- (133) Tao, R.; Sun, Z.; Li, F.; Fang, W.; Xu, L. Achieving Organic Metal Halide Perovskite into a Conventional Photoelectrode: Outstanding Stability in Aqueous Solution and High-Efficient Photoelectrochemical Water Splitting. *ACS Appl. Energy Mater.* **2019**, *2* (3), 1969–1976.
- (134) Kim, T. G.; Lee, J. H.; Hyun, G.; Kim, S.; Chun, D. H.; Lee, S.; Bae, G.; Oh, H.-S.; Jeon, S.; Park, J. H. Monolithic Lead Halide Perovskite Photoelectrochemical Cell with 9. 16% Applied Bias Photon-to-Current Efficiency. *ACS Energy Lett.* **2022**, *7* (1), 320–327.
- (135) Yang, M.-Z.; Xu, Y.-F.; Liao, J.-F.; Wang, X.-D.; Chen, H.-Y.; Kuang, D.-B. Constructing CsPbBr_xI_{3-x} Nanocrystal/Carbon Nanotube Composites with Improved Charge Transfer and Light Harvesting for Enhanced Photoelectrochemical Activity. *J. Mater. Chem. A* **2019**, *7* (10), 5409–5415.
- (136) Hamdan, M.; Chandiran, A. K. Cs₂PtI₆ Halide Perovskite Is Stable to Air, Moisture, and Extreme PH: Application to Photoelectrochemical Solar Water Oxidation. *Angew. Chem.* **2020**, *132* (37), 16167–16172.
- (137) Peng, H.; Xu, L.; Sheng, Y.; Sun, W.; Yang, Y.; Deng, H.; Chen, W.; Liu, J. Highly Conductive Ligand-Free Cs₂PtBr₆ Perovskite Nanocrystals with a Narrow Bandgap and Efficient Photoelectrochemical Performance. *Small* **2021**, *17* (38), 2102149.
- (138) Wang, X.-D.; Miao, N.-H.; Liao, J.-F.; Li, W.-Q.; Xie, Y.; Chen, J.; Sun, Z.-M.; Chen, H.-Y.; Kuang, D.-B. The Top-down Synthesis of Single-Layered Cs₄Cu₂Cl₁₂ Halide Perovskite Nanocrystals for Photoelectrochemical Application. *Nanoscale* **2019**, *11* (12), 5180–5187.
- (139) Wei, C.; Xu, Z. J. The Comprehensive Understanding of 10 MA Cm⁻²geo as an Evaluation Parameter for Electrochemical Water Splitting. *Small Methods* **2018**, *2* (11). DOI: [10.1002/smtd.201800168](https://doi.org/10.1002/smtd.201800168).
- (140) Poli, I.; Hintermair, U.; Regue, M.; Kumar, S.; Sackville, E. V.; Baker, J.; Watson, T. M.; Eslava, S.; Cameron, P. J. Graphite-Protected CsPbBr₃ Perovskite Photoanodes Functionalised with Water Oxidation Catalyst for Oxygen Evolution in Water. *Nat. Commun.* **2019**, *10* (1), 2097.
- (141) Gao, L.-F.; Luo, W.-J.; Yao, Y.-F.; Zou, Z.-G. An All-Inorganic Lead Halide Perovskite-Based Photocathode for Stable Water Reduction. *Chem. Commun.* **2018**, *54* (81), 11459–11462.
- (142) Dang, T. C.; Le, H. C.; Pham, D. L.; Nguyen, S. H.; Nguyen, T. T. O.; Nguyen, T. T.; Nguyen, T. D. Synthesis of Perovskite Cs₂SnI₆ Film via the Solution Processed Approach: First Study on the Photoelectrochemical Water Splitting Application. *J. Alloys Compd.* **2019**, *805*, 847–851.
- (143) Liu, M.; Pasanen, H.; Ali-Löytty, H.; Hiltunen, A.; Lahtonen, K.; Qudsia, S.; Smått, J.; Valden, M.; Tkachenko, N. V.; Vivo, P. B-Site Co-Alloying with Germanium Improves the Efficiency and Stability of All-Inorganic Tin-Based Perovskite Nanocrystal Solar Cells. *Angew. Chemie Int. Ed.* **2020**, *59* (49), 22117–22125.
- (144) Andrei, V.; Hoye, R. L. Z.; Crespo-Quesada, M.; Bajada, M.; Ahmad, S.; De Volder, M.; Friend, R.; Reisner, E. Scalable Triple Cation Mixed Halide Perovskite–BiVO₄ Tandems for Bias-Free Water Splitting. *Adv. Energy Mater.* **2018**, *8* (25). DOI: [10.1002/aenm.201801403](https://doi.org/10.1002/aenm.201801403).
- (145) Shi, R.; Waterhouse, G. I. N.; Zhang, T. Recent Progress in Photocatalytic CO₂ Reduction Over Perovskite Oxides. *Sol. RRL* **2017**, *1* (11). DOI: [10.1002/solr.201700126](https://doi.org/10.1002/solr.201700126).
- (146) Hori, Y.; Wakebe, H.; Tsukamoto, T.; Koga, O. Electrocatalytic Process of CO Selectivity in Electrochemical Reduction of CO₂ at Metal Electrodes in Aqueous Media. *Electrochim. Acta* **1994**, *39* (11–12), 1833–1839.
- (147) Andrei, V.; Ucoski, G. M.; Pornrungroj, C.; Uswachoke, C.; Wang, Q.; Achilleos, D. S.; Kasap, H.; Sokol, K. P.; Jagt, R. A.; Lu, H.; Lawson, T.; Wagner, A.; Pike, S. D.; Wright, D. S.; Hoye, R. L. Z.; MacManus-Driscoll, J. L.; Joyce, H. J.; Friend, R. H.; Reisner, E. Floating Perovskite-BiVO₄ Devices for Scalable Solar Fuel Production. *Nature* **2022**, *608* (7923), 518–522.
- (148) Andrei, V.; Jagt, R. A.; Rahaman, M.; Lari, L.; Lazarov, V. K.; MacManus-Driscoll, J. L.; Hoye, R. L. Z.; Reisner, E. Long-Term Solar Water and CO₂ Splitting with Photoelectrochemical BiOI–BiVO₄ Tandems. *Nat. Mater.* **2022**, *21* (8), 864–868.
- (149) Park, N.-G.; Zhu, K. Scalable Fabrication and Coating Methods for Perovskite Solar Cells and Solar Modules. *Nat. Rev. Mater.* **2020**, *5* (5), 333–350.
- (150) Chen, J.; Yin, J.; Zheng, X.; Ait Ahsaine, H.; Zhou, Y.; Dong, C.; Mohammed, O. F.; Takanabe, K.; Bakr, O. M. Compositionally Screened Eutectic Catalytic Coatings on Halide Perovskite Photocathodes for Photoassisted Selective CO₂ Reduction. *ACS Energy Lett.* **2019**, *4* (6), 1279–1286.
- (151) Zhang, H.; Chen, Y.; Wang, H.; Wang, H.; Ma, W.; Zong, X.; Li, C. Carbon Encapsulation of Organic–Inorganic Hybrid Perovskite toward Efficient and Stable Photo-Electrochemical Carbon Dioxide Reduction. *Adv. Energy Mater.* **2020**, *10* (44), 1–9.
- (152) Andrei, V.; Reuillard, B.; Reisner, E. Bias-Free Solar Syngas Production by Integrating a Molecular Cobalt Catalyst with Perovskite–BiVO₄ Tandems. *Nat. Mater.* **2020**, *19* (2), 189–194.
- (153) Jun, S. E.; Lee, J. K.; Ryu, S.; Jang, H. W. Single Atom Catalysts for Photoelectrochemical Water Splitting. *ChemCatChem.* **2023**, *15* (21), No. e202300926.

- (154) Zhao, Y.; Niu, Z.; Zhao, J.; Xue, L.; Fu, X.; Long, J. Recent Advancements in Photoelectrochemical Water Splitting for Hydrogen Production. *Electrochim. Energy Rev.* **2023**, *6* (1), 14.
- (155) Liu, Y.; Li, W.; Xia, Y. Recent Progress in Polyanionic Anode Materials for Li (Na)-Ion Batteries. *Electrochim. Energy Rev.* **2021**, *4* (3), 447–472.
- (156) Shi, J.; Zhao, X.; Li, C. Surface Passivation Engineering for Photoelectrochemical Water Splitting. *Catalysts* **2023**, *13* (2), 217.
- (157) Zhang, Y.; Zhou, S.; Sun, K. Cu₂ZnSnS₄ (CZTS) for Photoelectrochemical CO₂ Reduction: Efficiency, Selectivity, and Stability. *Nanomaterials* **2023**, *13* (20), 2762.
- (158) Li, Y.; Li, S.; Huang, H. Metal-Enhanced Strategies for Photocatalytic and Photoelectrochemical CO₂ Reduction. *Chem. Eng. J.* **2023**, *457*, No. 141179.
- (159) Zhang, Q.; Wang, Z.; He, H.; Wang, J.; Zhao, Y.; Zhang, X. Photoelectrochemical and Electrochemical CO₂ Reduction to Formate on Post-Transition Metal Block-Based Catalysts. *Sustain. Energy Fuels* **2023**, *7* (11), 2545–2567.
- (160) Thakur, A.; Ghosh, D.; Devi, P.; Kim, K.-H.; Kumar, P. Current Progress and Challenges in Photoelectrode Materials for the Production of Hydrogen. *Chem. Eng. J.* **2020**, *397*, No. 125415.
- (161) Singh, P. K.; Kaushik, R.; Halder, A. Photoelectrochemical CO₂ Reduction: Perspective and Challenges. In *Handbook of Green and Sustainable Nanotechnology: Fundamentals, Developments and Applications*; Springer International Publishing: Cham, 2023; pp 613–639. DOI: [10.1007/978-3-031-16101-8_89](https://doi.org/10.1007/978-3-031-16101-8_89).
- (162) Wang, S.; Wang, A.; Hao, F. Toward Stable Lead Halide Perovskite Solar Cells: A Knob on the A/X Sites Components. *iScience* **2022**, *25* (1), No. 103599.
- (163) Wang, Q.; Phung, N.; Di Girolamo, D.; Vivo, P.; Abate, A. Enhancement in Lifespan of Halide Perovskite Solar Cells. *Energy Environ. Sci.* **2019**, *12* (3), 865–886.
- (164) Odabaşı, Ç.; Yıldırım, R. Machine Learning Analysis on Stability of Perovskite Solar Cells. *Sol. Energy Mater. Sol. Cells* **2020**, *205*, No. 110284.
- (165) Wang, M.; Li, Y.; Cui, X.; Zhang, Q.; Pan, S.; Mazumdar, S.; Zhao, Y.; Zhang, X. High-Performance and Stable Perovskite-Based Photoanode Encapsulated by Blanket-Cover Method. *ACS Appl. Energy Mater.* **2021**, *4* (8), 7526–7534.
- (166) Ahmad, S.; Sadhanala, A.; Hoye, R. L. Z.; Andrei, V.; Modarres, M. H.; Zhao, B.; Rongé, J.; Friend, R.; De Volder, M. Triple-Cation-Based Perovskite Photocathodes with AZO Protective Layer for Hydrogen Production Applications. *ACS Appl. Mater. Interfaces* **2019**, *11* (26), 23198–23206.
- (167) Kim, I. S.; Pellin, M. J.; Martinson, A. B. F. Acid-Compatible Halide Perovskite Photocathodes Utilizing Atomic Layer Deposited TiO₂ for Solar-Driven Hydrogen Evolution. *ACS Energy Lett.* **2019**, *4* (1), 293–298.
- (168) Yilmaz, B.; Odabaşı, Ç.; Yıldırım, R. Efficiency and Stability Analysis of 2D/3D Perovskite Solar Cells Using Machine Learning. *Energy Technol.* **2022**, *10* (3), 1–12.
- (169) Jiang, X.; Fu, X.; Ju, D.; Yang, S.; Chen, Z.; Tao, X. Designing Large-Area Single-Crystal Perovskite Solar Cells. *ACS Energy Lett.* **2020**, *5* (6), 1797–1803.
- (170) Murali, B.; Kolli, H. K.; Yin, J.; Ketavath, R.; Bakr, O. M.; Mohammed, O. F. Single Crystals: The Next Big Wave of Perovskite Optoelectronics. *ACS Mater. Lett.* **2020**, *2* (2), 184–214.
- (171) Zhang, X.; Zhang, R.; Yang, T.; Cheng, Y.; Li, F.; Li, W.; Huang, J.; Liu, H.; Zheng, R. Facile Fabrication of Hybrid Perovskite Single-Crystalline Photocathode for Photoelectrochemical Water Splitting. *Energy Technol.* **2021**, *9* (5), 1–8.
- (172) Kim, J.; Seo, S.; Lee, J.; Choi, H.; Kim, S.; Piao, G.; Kim, Y. R.; Park, B.; Lee, J.; Jung, Y.; Park, H.; Lee, S.; Lee, K. Efficient and Stable Perovskite-Based Photocathode for Photoelectrochemical Hydrogen Production. *Adv. Funct. Mater.* **2021**, *31* (17), 1–9.
- (173) Metrangolo, P.; Canil, L.; Abate, A.; Terraneo, G.; Cavallo, G. Halogen Bonding in Perovskite Solar Cells: A New Tool for Improving Solar Energy Conversion. *Angew. Chem.* **2022**, *134* (11), No. e202114793.
- (174) Bonabi Naghadeh, S.; Luo, B.; Abdelmageed, G.; Pu, Y.-C.; Zhang, C.; Zhang, J. Z. Photophysical Properties and Improved Stability of Organic-Inorganic Perovskite by Surface Passivation. *J. Phys. Chem. C* **2018**, *122* (28), 15799–15818.
- (175) Ma, F.; Zhao, Y.; Qu, Z.; You, J. Developments of Highly Efficient Perovskite Solar Cells. *Accounts Mater. Res.* **2023**, *4* (8), 716–725.
- (176) Zhu, H.; Teale, S.; Lintangpradipto, M. N.; Mahesh, S.; Chen, B.; McGehee, M. D.; Sargent, E. H.; Bakr, O. M. Long-Term Operating Stability in Perovskite Photovoltaics. *Nat. Rev. Mater.* **2023**, *8* (9), 569–586.
- (177) Agarwal, A.; Goverapet Srinivasan, S.; Rai, B. Data-Driven Discovery of 2D Materials for Solar Water Splitting. *Front. Mater.* **2021**, *8*, 1–12.
- (178) Zhang, X.; Zhang, Z.; Wu, D.; Zhang, X.; Zhao, X.; Zhou, Z. Computational Screening of 2D Materials and Rational Design of Heterojunctions for Water Splitting Photocatalysts. *Small Methods* **2018**, *2* (5), No. 1700359.
- (179) Zhang, L.; Hu, W.; He, M.; Li, S. Optimizing Photoelectrochemical Photovoltage and Stability of Molecular Interlayer-Modified Halide Perovskite in Water: Insights from Interpretable Machine Learning and Symbolic Regression. *ACS Appl. Energy Mater.* **2023**, *6* (10), 5177–5187.
- (180) Pan, Z.; Zhou, Y.; Zhang, L. Photoelectrochemical Properties, Machine Learning, and Symbolic Regression for Molecularly Engineered Halide Perovskite Materials in Water. *ACS Appl. Mater. Interfaces* **2022**, *14* (7), 9933–9943.
- (181) Kumar, A.; Singh, S.; Mohammed, M. K. A.; Sharma, D. K. Accelerated Innovation in Developing High-Performance Metal Halide Perovskite Solar Cell Using Machine Learning. *Int. J. Mod. Phys. B* **2023**, *37* (07), No. 2350067.
- (182) Meftahi, N.; Surmiak, M. A.; Fürer, S. O.; Rietwyk, K. J.; Lu, J.; Raga, S. R.; Evans, C.; Michalska, M.; Deng, H.; McMeekin, D. P.; Alan, T.; Vak, D.; Chesman, A. S. R.; Christofferson, A. J.; Winkler, D. A.; Bach, U.; Russo, S. P. Machine Learning Enhanced High-Throughput Fabrication and Optimization of Quasi-2D Ruddlesden-Popper Perovskite Solar Cells. *Adv. Energy Mater.* **2023**, *13* (38), No. 2203859.
- (183) Lu, Y.; Wei, D.; Liu, W.; Meng, J.; Huo, X.; Zhang, Y.; Liang, Z.; Qiao, B.; Zhao, S.; Song, D.; Xu, Z. Predicting the Device Performance of the Perovskite Solar Cells from the Experimental Parameters through Machine Learning of Existing Experimental Results. *J. Energy Chem.* **2023**, *77*, 200–208.
- (184) Odabaşı, Ç.; Yıldırım, R. Assessment of Reproducibility, Hysteresis, and Stability Relations in Perovskite Solar Cells Using Machine Learning. *Energy Technol.* **2020**, *8* (12), No. 1901449.
- (185) Odabaşı, Ç.; Yıldırım, R. Performance Analysis of Perovskite Solar Cells in 2013–2018 Using Machine-Learning Tools. *Nano Energy* **2019**, *56*, 770–791.
- (186) Levin, I. *NIST Inorganic Crystal Structure Database (ICSD)*; National Institute of Standards and Technology; DOI: [10.18434/M32147](https://doi.org/10.18434/M32147).
- (187) Jain, A.; Ong, S. P.; Hautier, G.; Chen, W.; Richards, W. D.; Dacek, S.; Cholia, S.; Gunter, D.; Skinner, D.; Ceder, G.; Persson, K. A. Commentary: The Materials Project: A Materials Genome Approach to Accelerating Materials Innovation. *APL Mater.* **2013**, *1* (1), No. 011002.
- (188) Alharbi, F. H.; Rashkeev, S. N.; El-Mellouhi, F.; Lüthi, H. P.; Tabet, N.; Kais, S. An Efficient Descriptor Model for Designing Materials for Solar Cells. *npj Comput. Mater.* **2015**, *1* (1), 15003.
- (189) Curtarolo, S.; Setyawan, W.; Hart, G. L. W.; Jahnatek, M.; Chepulskii, R. V.; Taylor, R. H.; Wang, S.; Xue, J.; Yang, K.; Levy, O.; Mehl, M. J.; Stokes, H. T.; Demchenko, D. O.; Morgan, D. AFLOW: An Automatic Framework for High-Throughput Materials Discovery. *Comput. Mater. Sci.* **2012**, *58*, 218–226.
- (190) Draxl, C.; Scheffler, M. The NOMAD Laboratory: From Data Sharing to Artificial Intelligence. *J. Phys. Mater.* **2019**, *2* (3), No. 036001.

- (191) Zhang, Q.; Zhang, Q.; Shi, W.; Zhong, H. Firework: Data Processing and Sharing for Hybrid Cloud-Edge Analytics. *IEEE Trans. Parallel Distrib. Syst.* **2018**, *29* (9), 2004–2017.
- (192) Mathew, K.; Montoya, J. H.; Faghaninia, A.; Dwarakanath, S.; Aykol, M.; Tang, H.; Chu, I.; Smidt, T.; Bocklund, B.; Horton, M.; Dagdelen, J.; Wood, B.; Liu, Z.-K.; Neaton, J.; Ong, S. P.; Persson, K.; Jain, A. Atomate: A High-Level Interface to Generate, Execute, and Analyze Computational Materials Science Workflows. *Comput. Mater. Sci.* **2017**, *139*, 140–152.
- (193) Ong, S. P.; Richards, W. D.; Jain, A.; Hautier, G.; Kocher, M.; Cholia, S.; Gunter, D.; Chevrier, V. L.; Persson, K. A.; Ceder, G. Python Materials Genomics (Pymatgen): A Robust, Open-Source Python Library for Materials Analysis. *Comput. Mater. Sci.* **2013**, *68*, 314–319.
- (194) Jao, M.-H.; Chan, S.-H.; Wu, M.-C.; Lai, C.-S. Element Code from Pseudopotential as Efficient Descriptors for a Machine Learning Model to Explore Potential Lead-Free Halide Perovskites. *J. Phys. Chem. Lett.* **2020**, *11* (20), 8914–8921.
- (195) Liang, G.-Q.; Zhang, J. A Machine Learning Model for Screening Thermodynamic Stable Lead-Free Halide Double Perovskites. *Comput. Mater. Sci.* **2022**, *204*, No. 111172.
- (196) Gao, Z.; Zhang, H.; Mao, G.; Ren, J.; Chen, Z.; Wu, C.; Gates, I. D.; Yang, W.; Ding, X.; Yao, J. Screening for Lead-Free Inorganic Double Perovskites with Suitable Band Gaps and High Stability Using Combined Machine Learning and DFT Calculation. *Appl. Surf. Sci.* **2021**, *568*, No. 150916.
- (197) Wang, T.; Fan, S.; Jin, H.; Yu, Y.; Wei, Y. Substitution Engineering of Lead-Free Halide Perovskites for Photocatalytic Applications Assisted by Machine Learning. *Phys. Chem. Chem. Phys.* **2023**, *25* (17), 12450–12457.
- (198) Burger, B.; Maffettone, P. M.; Gusev, V. V.; Aitchison, C. M.; Bai, Y.; Wang, X.; Li, X.; Alston, B. M.; Li, B.; Clowes, R.; Rankin, N.; Harris, B.; Sprick, R. S.; Cooper, A. I. A Mobile Robotic Chemist. *Nature* **2020**, *583* (7815), 237–241.
- (199) Ahmadi, M.; Ziatidinov, M.; Zhou, Y.; Lass, E. A.; Kalinin, S. V. Machine Learning for High-Throughput Experimental Exploration of Metal Halide Perovskites. *Joule* **2021**, *5* (11), 2797–2822.
- (200) Dubey, A.; Sanchez, S. L.; Yang, J.; Ahmadi, M. Lead-Free Halide Perovskites for Photocatalysis via High-Throughput Exploration. *Chem. Mater.* **2024**, *36* (5), 2165–2176.
- (201) Rahmani, S.; Rezaei, M.; Meshkani, F. Preparation of Highly Active Nickel Catalysts Supported on Mesoporous Nanocrystalline γ -Al₂O₃ for CO₂Methanation. *J. Ind. Eng. Chem.* **2014**, *20* (4), 1346–1352.
- (202) Liu, S. F.; Liu, Y.; Zhu, X.; Feng, J.; Yang, Z.; Zhao, K.; Yang, D. Perovskite—A Wonder Material for Photovoltaic and Optoelectronic Applications. In *Proceedings of the 2018 IEEE 7th World Conference on Photovoltaic Energy Conversion (WCPEC)* (A Joint Conference of 45th IEEE PVSC, 28th PVSEC & 34th EU PVSEC); IEEE, 2018; pp 3503–3505..